NTNU
Norwegian University of
Science and Technology

Modelling of Ground Source Systems for Heat Pump Operations

Hongyun Zhou

Sustainable Energy
Submission date: December 2017
Supervisor: Trygve Magne Eikevik, EPT

Norwegian University of Science and Technology
Department of Energy and Process Engineering

Preface

This thesis is presented as a fulfillment of the requirement for Master degree at Shanghai Jiao Tong University (SJTU) and Norwegian University of Science and Technology (NTNU), Trondheim, Norway.

Work was carried out under the main objective of establishing a credible model for regional underground hydraulic and thermal simulation in city Melhus, Norway. Multiple external factors were tested for their own influence on both breakthrough time and long-term efficiency. Hence recommendations and feasible solutions for owners to utilize the system and delay the adverse impact brought by the hydraulic and thermal interaction between wells were accordingly projected.

The work is carried out at the department of Energy and Process Engineering (EPT). Gratitude shall be paid to my advisor Prof. Trygve M. Eikevik, Prof. Li, Research Advisor Randi for instruction and PhD candidate Sondre for the providing crucial data for performing simulation.

Abstract

This thesis concerns the regional hydraulic and thermal interference between well doublets of ground source heat pump systems. The thesis falls into three parts of which the first focus on theoretical review of operating mechanism and available modelling methodology of ground source heat pump systems. The second part emphasize on establishing appropriate model to reflect the interference with experimental data collected from real sites at city Melhus, Norway. The third and last part involves a test for validation and simulation result analysis for drawing suggestions to help mitigate the negative interference between wells doublets. The essence of the thesis is described hereunder, starting with the ground source heat pump systems.

A Ground source heat pump (GSHP) system migrates the heat from the outdoor circuit to the air conditioning and hot water terminal of indoor circuit through a circular operation of refrigerant circuit. Groundwater heat pump (GWHP) systems, as an open-loop subclass of Ground source heat pump systems take aquifers as a storage of thermal energy. The system operates by drawing water from an abstraction well, passing it through a heat exchanger and discharging it into nearby infiltration well.

From the point of either users or regulatory authority, ground source heat pump systems have incomparable advantages over conventional heating approaches in reproducibility, energy conservation, environmental friendliness, versatility and long service life. Likewise, groundwater source heat pump systems also yield a higher performance efficiency and lower operation cost than Air source heat pump (ASHP) systems. To help achieve a higher overall efficiency during the systems' service life, numerous models have being proposed by researchers to predict the thermal response under different design parameters and groundwater flow conditions.

As for city Melhus, wells for groundwater source heat pump system are sporadically distributed in its urban area. Meanwhile the geological condition of layer of aquifers in Melhus fits the case of unconfined aquifers and strata structure could be simplified into five major layers according to predominating constituent of each layer. A numerical model was therefore established by software Feflow on the basis of parameters collected from samples at city fire station.

Validation was conducted and the outcomes were compared to theoretical and experimental data. Series of 10-year simulations were performed. Simulations disclosed the pros and cons of multiple means of figuring out hydraulic and thermal breakthrough time, two crucial indicators to reflect the moment when overall efficiency of the system begins to deteriorate. Besides, the outcomes also revealed to which extent breakthrough time and system's overall efficiency could be affected by altering the external factors used as independent variables of input. It was found that:

Placing the abstraction well up the hydraulic gradient from the infiltration well thus forming a contrary flow would produce a 3.4% increment in thermal breakthrough time as compared to same hydraulic gradient's case and placing it down the hydraulic gradient would produce a 2.9% depletion on thermal breakthrough time in contrast. Doubling the speed of groundwater flow would yield a 3.3% increment in thermal breakthrough time. Reducing the abstraction rate or hydraulic conductivity by half would generate a 107.5%, 80.2% increment in thermal breakthrough time, representing a negative correlation. From this point of view, abstraction rate along with hydraulic conductivity proves to play more significant a role in affecting breakthrough time than direction or speed of groundwater flow.

In addition to breakthrough time, the same factors also contribute to the movement of turning point for operational efficiency. Meanwhile, setting the abstraction point higher than or at least at the same depth of injection level would gain a long-term advantage over setting it 5 meters below the injection level. Factors like direction and speed of groundwater flow contributes limited influence while abstraction rate and hydraulic conductivity both would incur a remarkable shift on transient and overall efficiency turning point. Compared to a normal service life of the groundwater source heat pump system, users are only required to make a trade-off between short-term and long-term efficiency only if the abstraction rate is smaller than 7.5L per second or the specific horizontal hydraulic conductivity is below 0.002m/s.

Furthermore, users are recommended to turn the GWHP system into intermittent operation. Put the system in operation in an intermittent manner would significantly raise the ending temperature at the end of each operation cycle by 0.2-0.4 degrees Celsius and substantially delay the breakthrough. Meanwhile, intermittent operation also contributes to a postpone of the turning point of the overall efficiency. Under such circumstance, users are more likely to be

obliged to choose between the short-term and long-term efficiency.

Acknowledgements

My first sincere appreciation goes to my advisor Prof. Li. Prof Li has been my advisor for over 4 years. Prof Li has always been an unparalleled advisor with profound attainments. It was him who led to the field and pass on the skills and spirit for conducting research. Whenever I encounter hardship in either simulation or writing a report, Prof Li always spares his time to help.

Supreme gratitude shall also be paid to my main advisor Prof. Trygve M. Eikevik who has been always kind and helpful. However busy he is, Prof. Trygve adhere to a routine meeting on which he provided crucial advices and support on dealing with thorny problems. It was him who repeatedly called MIKE Norway to arrange the necessary conditions for the download and license for Feflow software and provided practical suggestions when I met problems of erratic experimental data.

I would express my gratitude to my Research Advisor Randi for her instruction. Prof. Randi made my reply on project report, invited me to the half-day seminar on groundwater and heat pumps in Melhus center and drived us around for visiting the sporadically distributed wells in Melhus.

I would also like to thank my senior Zhequan for his guidance and instruction. I used to send my semi-finished report to Zhequan for consultation before handed in to my professors; PhD candidate Sondre for the providing essential data for performing simulation; my peer Chengyang for tackling troublesome daily affairs like opening the bank account; Anja and other friends I've made in the colleagues at NTNU for teaching me a few words of Norwegian and presenting me a brand new angle to understand Scandinavian culture from locals' perspective.

Table of Contents

List of figures

List of tables

Nomenclature

Symbol	Name	Unit	Symbol	Name	Unit
S	Storage coefficient	-	λ	Thermal conductivity	$Wm^{-1}K^{-1}$
S_S	Specific storage	m^{-1}	λ_{eff}	Effective thermal conductivity	$Wm^{-1}K^{-1}$
S_Y	Specific yield	-	g	Acceleration due to gravity	m^2s^{-1}
V_w	Volume of water released from storage	m^3	R_w	Well radius	m
D	Thickness of aquifer	m	G	Heat rejection	J
A	Sectional area	m^2	c	Heat absorption	J
w	Width of aquifer	m	θ	Temperature	K
L	Well separation	m	θ_0	Initial temperature	K
h	Hydraulic head	m	θ_{gout}	Abstraction temperature	K
h_0	Initial hydraulic head	m	S_{VCwat}	Volumetric heat capacity of water	$Jm^{-3}K^{-1}$
Δh	Head difference between injection and abstraction well		S_{VCaq}	Volumetric heat capacity of aquifer	$Jm^{-3}K^{-1}$
$\frac{dh}{dx}$	Hydraulic gradient	-	SPF_c	Seasonal performance factor for the cooling system	-
i	Natural hydraulic gradient	-	C	Specific heat capacity	$Jkg^{-1}K^{-1}$
i_{rev}	Reverse hydraulic gradient between the two wells		v_D	Darcy velocity	ms^{-1}
			v	Velocity	ms^{-1}

n	Porosity	%	t_{hyd}	Hydraulic breakthrough time	s
n_e	Effective porosity	%	f_{recirc}	Recirculated proportion	%
K	Hydraulic conductivity	ms^{-1}	R_{the}	Thermal retardation factor	-
Z	Groundwater abstraction rate	$m^3\ s^{-1}$	T_{the}	Thermal breakthrough time	s
T	Transmissivity	$m^2\ s^{-1}$	s	Drawdown	m
T_f	Transmissivity of a fracture	$m^2 s^{-1}$	t	Time	s
b_a	Aperture	m	n	Surface normal vector	-
ρ	Density	kgm^{-3}	s	Surface area	m^2
ρ_w	Density of water	kgm^{-3}	V	volume	m^3
μ	Viscosity	$kgs^{-1}\ m^{-1}$	ε	Error	
μ_w	Dynamic viscosity of water	$kgs^{-1}\ m^{-1}$			

1. Introduction

A ground source heat pump (GSHP) system is a set of equipment taking the advantage of inverse Carnot cycle to provide space heating and cooling and domestic hot water for both residential and commercial usage. Since underground temperature is more stable a temperature than surface temperature, underground medium can serve as an ideal low-grade heat source in winter and heat sink in summer. Therefore a shorter lift (the difference between heat source and heat sink) of GSHP systems within the energy cycle ensures a relatively higher Coefficient of performance for air-conditioning compared to Air source heat pump (ASHP) systems.

The earliest recorded concept of using ground as heat source for heat pump was found in Swiss in 1912 (Ball et al., 1983). The technology remains undervalued late until 1950s when it swiftly drew the interest of researchers in North America and northern Europe (Ingersoll et al., 1954). Scandinavian countries focus more on winter heating while middle-latitude countries like the U.S. and China took both heating and cooling into consideration. Over the past five years, the world has witnessed an 8.65% and 10.3% ongoing growth per year in installed capacity of GSHP systems and energy utilized respectively (49898MWt and 325028TJ/a in 2015, World Geothermal Congress, 2015). China, meanwhile, generates an average 27% growth per year (National Bureau of Statics of China, 2015) and accounts for 23.61% of energy utilized by means of GSHP systems worldwide in 2015.

As is a booming industry worldwide, the modelling of ground source heat pump systems is of unique importance for it might provide owners with decision-making reference in choosing critical parameters like where to drill and the depth to drill so as not to introduce the unwanted interference between wells.

The report begins with a brief introduction of the overall operating mechanism, classification and potential merits of adopting GSHP systems. This is followed by a detailed discussion on hydraulic and thermal theories of Ground water heat pump system (GWHP). A literature review concerning different strategies of establishing models for both Ground coupled heat pump (GCHP) and GWHP systems is presented. And consequently, appropriate models to reflect regional hydraulic and heat transfer process between wells were established based on the geological data collected from the site in city Melhus. Meanwhile, methodology of modelling

went through validation with experimental data collected at Melhus fire station. Eventually, simulation results based on the models are abstracted and carefully analyzed; External factors were tested by variable controlling method and influence was recorded. Suggestions based on the results were drawn to help resolve the negative interference between well doublets in city Melhus.

2. Objectives

The objective of this work is to:

Perform a literature review of ground source systems.

Develop a simulation model for ground source heat pump system.

Plan and perform measurements to the system and verify the model

Make simulation of the influence of selected case studies

Make proposal for users' application.

3. Theory

3.1 Theory of GSHP systems

3.1.1 Operating Mechanism of ground source heat pump systems

An integrate GSHP system as is shown in figure 1 is commonly composed of three necessary circuits, i.e. outdoor circuit, refrigerant circuit and indoor circuit. In an outdoor circuit, high density polyethylene pipes are positioned beneath the ground forming an open loop with groundwater or a closed loop within which antifreeze fluid circulates. In a refrigerant circuit under heating mode, the compressor draws out refrigerant vapor and endows the vapor high pressure and temperature. The vapor is condensed in a condenser and reject considerable amount of heat to Heat-medium water in the Indoor circuit. Vapor condensed then experience a decompression process in the expansion valve, transformed into refrigerant liquid of low pressure and eventually absorbs heat from the Outdoor circuit in the evaporator. In an indoor circuit, heat absorbed is provided to terminal users by means of space heating and domestic hot water. On the whole, a GSHP system migrates the heat from the outdoor circuit to the air conditioning and hot water terminal of indoor circuit through the operation of refrigerant circuit.

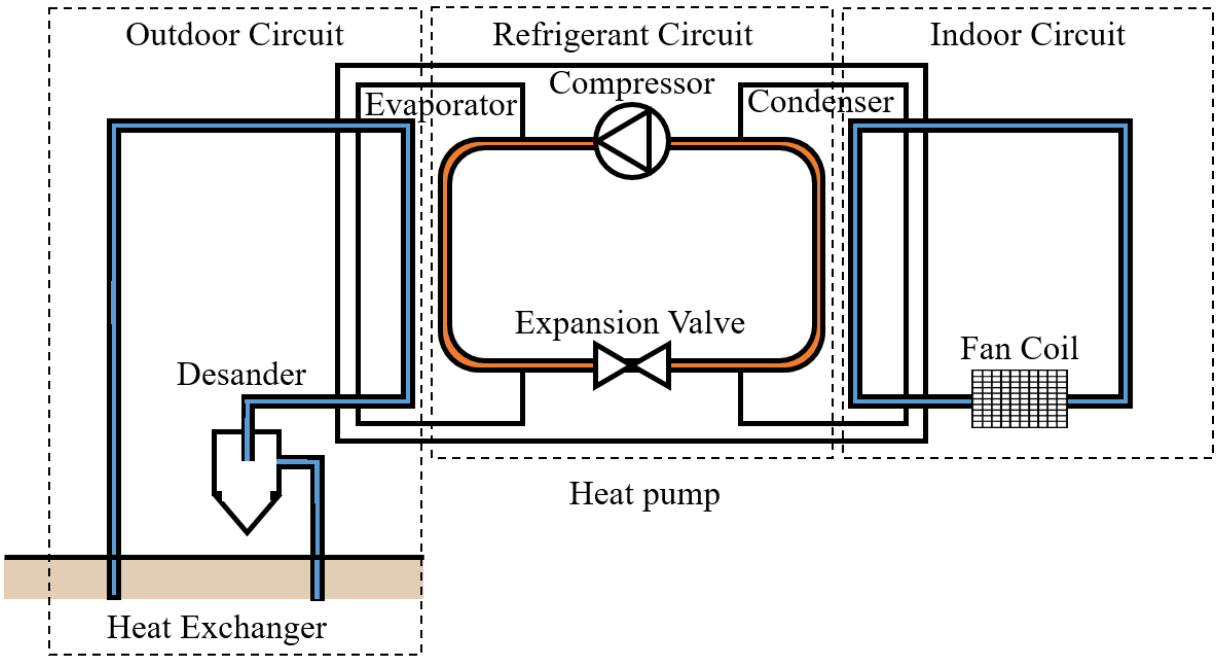

Figure 1: The operating cycle of a GSHP system

3.1.2 Classification of ground source heat pump systems

Based on the configuration of heat exchangers, ground source heat pump systems can be largely divided into three major categories by ASHRAE (Ball et al., 1983) as is shown in Figure 2.

Ground water heat pump systems (GWHP) adopt groundwater as an effective heat source. In most cases, groundwater is drawn from a production well, goes through a heat transfer process with heat pump evaporator and finally drained or pumped back to an infiltration well. GWHP systems are easily applicable if there is groundwater available in the vicinity. As long as temperature, quality and the amount of underlying groundwater meets the requirement, wells can be drilled with a minimal demand for ground surface area and relatively low initial investment (Kavanaugh, 1998). Hence the specific systems particularly apply to large individual buildings and compact building blocks. Despite of the advantages, GWHP systems have several deficiencies of nature. It's usually costly to maintain the systems due to the problem of clogging and potential fouling corrosion. Besides, the application of GWHP systems is occasionally vulnerable to various national policies for groundwater resources.

Surface water heat pump (SWHP) systems operate by having pipes placed at sufficient depth in a lake or reservoir. This help forms an open or closed loop system with massive water body and consequently promotes heat transfer efficiency by means of natural convection. The primary imperfection for the systems is the acrid demand for nearby water body and susceptible surface water temperature be subjected to changing climate.

Ground coupled heat pump (GCHP) systems are equipped with borehole heat exchangers (BHEs) buried underground within which fluid circulates in a closed loop and transfer heat to the evaporator. In addition, GCHP systems can be further classified to horizontal ones, vertical ones and slinky ones on account of different arrangements of heat exchangers. In a horizontal system, BHEs are arranged in parallel to each other in shallow stratum. Despite the fact that horizontal systems made up about half of the installations by 1995 (Kavanaugh et al., 1995), they are easily affected by changing air temperature and requires far more ground surface areas compared to other GCHP systems. In a vertical GCHP system, dozens of heat exchangers are installed in the boreholes refilled with grout which is intentionally treated to prevent water contamination and assist heat transfer. Since GCHP systems do not need to drain aquifers, they can be universally used in areas with inferior hydrogeological conditions. Moreover, the

systems pose no threat on both contamination and surface subsidence by the overuse of groundwater. Therefore, GCHP systems naturally incur less policy intervention from relevant administrative departments.

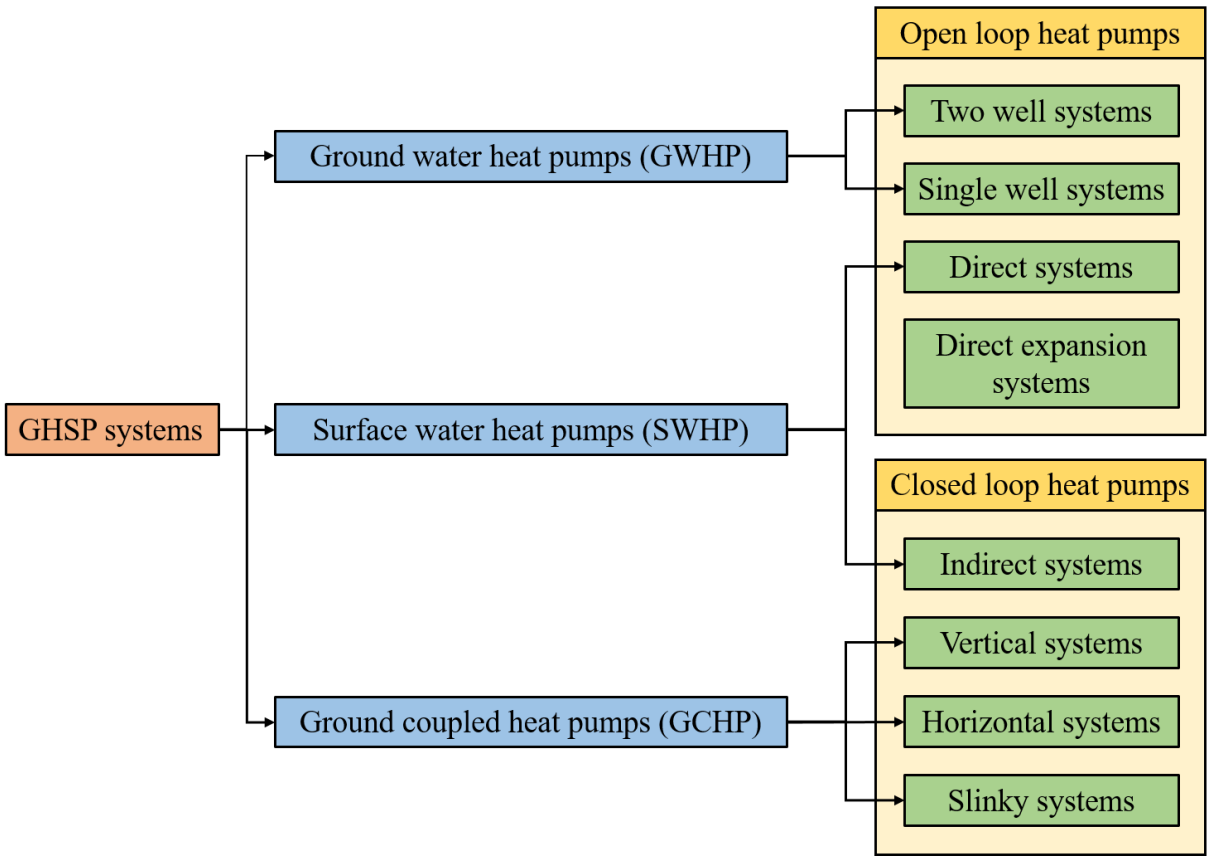

Figure 2: Classification of GSHP system (Source: The Geo-Heat Center's Survival Kit for the Prospective Geothermal Heat Pump Owner)

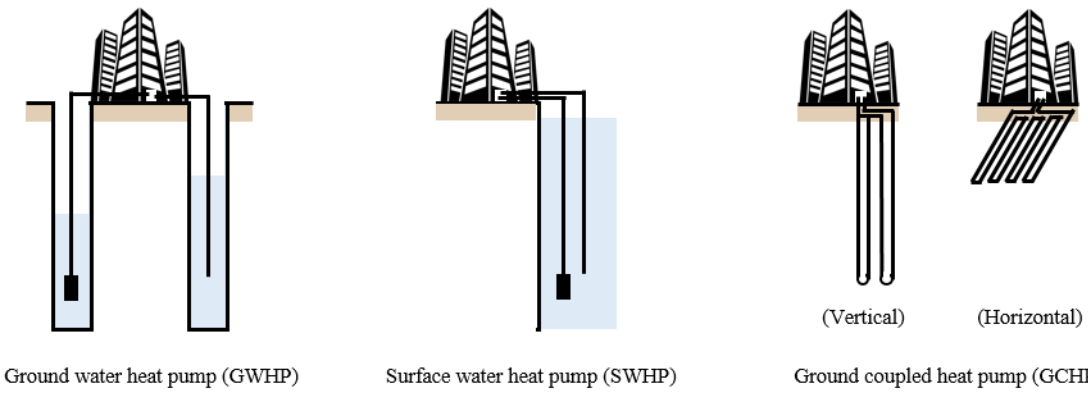

Figure 3: Schematics of major types of ground source heat pumps (Source: Vertical-borehole ground-coupled heat pumps: a review of models and systems)

3.1.3 Difference between GSHP systems and ASHP systems

ASHP systems are basically air-source heat pumps removing heat from the external air to indoor environment. In comparison, GSHP systems acquire heat from underground which has more stable a temperature throughout a year (Carslaw and Jaeger, 1959) and less affected by the changing climate. Since a warmer temperature of the heat source in winter as well as a cooler temperature of the heat sink in summer plays an identical role in reducing the temperature lift of the heat pump, GSHP systems always ensure a relatively higher efficiency and lower energy consumption regardless of the season. Apart from a higher efficiency, GSHP systems do not have an outdoor unit and above all create no excess burdens on heat island effect in urban areas (Shonder et al., 1999).

3.2 Potential merits of GSHP systems

GSHP technology is a reproducible technique of utilizing the abundant low-temperature geothermal resources reserved in the shallow subsurface of ground. As is mentioned in former chapter, GSHP technology also has an advantage in energy conservation in virtue of a higher COP. According to U.S. Environmental Protection Agency (EPA), a well-designed GSHP system can save people 30-40% of expense for air-conditioning. Besides, GSHP technology is comparatively more environment friendly. An ASHP systems typically accompanies problem of refrigerant dissipation. In contrast, A GSHP system involve less consumption of refrigerant and consequently lower probability of leakage. From this perspective, GSHP systems are more favorable in community. Apart from environmental concerns, GSHP systems have a wide range of versatility. It can provide domestic hot water as well as space heating and is applicable in the overwhelming majority of buildings and houses. Finally, a well-maintained GSHP system has an operational lifetime of 20-25 years, slightly longer than the service life of a traditional central air-conditioner (CAC). In brief, GSHP technology has incomparable advantages in reproducibility, energy conservation, environmental friendliness, versatility and long lifetime. A specific table of economic and environmental benefits is given as follows.

Table 1: Economic and environmental benefits (Source: Operating cost report of Ground source heat pump system, HOMEWELLER) (kgce: energy consumed represented by 1 kg of standard

coal)

Economic Benefits							
		Heat pump Approaches			Conventional heating Approaches		
		GCHP	GWHP	ASHP	Coal-Burning Boiler	Gas Boiler	Electric heating
Primary Energy Ratio (%)		119	106	99	69	90	33
Initial Investment (yuan/m^2)		240~360	180~260	220~260	50~80	80~160	80~120
Heating season	Operation cost	7~14	12~18	16~19	23~26	27~30	58~61
	Energy consumption (kgce/m^2)	10.96	12.33	13.15	19.92	15.21	39.46
	Carbon dioxide emissions (kg/m^2)	18.03	20.12	22.19	33.61	22.17	66.56
Environmental Benefits (Compared to energy produced by Coal-Burning Boiler)							
Heating season	Energy saved in kgce (kgce/m^2)	8.96	7.59	6.77	0	4.71	-19.53
	Carbon dioxide emission reductions (kg/m^2)	15.12	12.81	11.42	0	7.95	-32.95
	Sulfur dioxide emission reductions (kg/m^2)	0.2	0.17	0.15	0	0.1	-0.43
	Average energy saving rate (%)	46.99	38.11	33.99	0	23.64	-98.03

4. Theory of GWHP systems

A GWHP system is a kind of open-loop GSHP system depending on the existence of an aquifer to support the required heating and cooling load of the system. An aquifer is an underground layer of water-bearing permeable rock, rock fractures or unconsolidated materials (gravel, sand, or silt) from which groundwater can be mined (Wikipedia, 2010). Unlike GCHP systems which extract heat from segregate heat carrying fluid in BHEs, GWHP systems directly pump groundwater at a certain temperature from the wells to the surface.

The result is cold or warm plumes develop through the process of infiltration yet it could be mitigated by lateral conductive heat transport and by convection of groundwater flow. To help design and install the systems, heat transfer process in the subsurface ought to be appropriately characterized to avoid the potential thermal feedbacks. Thereafter, individual and collective sustainability of the GWHP systems can be examined and suggestions can be given accordingly.

4.1 Common design flaws regarding GWHP systems

1. Input parameters are not precise enough.
2. Over-optimism regarding the hydraulic properties of aquifers.
3. Improper oversight of wastage, maintenance, dissolved gas, chemical and microbiological reactions.
4. Fail to take hydraulic and thermal breakthrough into consideration.

All these flaws (Banks D., 2012) might contribute a biased prediction of the efficiency and sustainability of individual and monolithic systems. Since point 1, 2 and 3 can all be resolved by meticulous investigation, we'll mainly focus on point 4, i.e. the compromising influence on thermal efficiency and sustainability of system by having the water reinjected flow back into the abstraction well.

4.2 Aquifer characteristic

Confined and unconfined aquifers are two separate end members of aquifers (Banks D., 2012). Confined aquifers are aquifers overlain by a low-permeability confining layer known as aquitard. Unconfined aquifers, on the other hand, are exposed to an upper boundary of free

water surface called water table. Although the difference between confined and unconfined aquifers is not geologically significant, they have distinctive characteristics as follows,

For a confined aquifer:

1. It's usually held under excess pressure and groundwater head is higher than the top of the aquifer.
2. It's transmissivity T is usually a constant
3. Has low specific storage (S_S as little as 10^{-5})
4. The thickness of aquifer D can change on the basis of seasonal precipitation.

For an unconfined aquifer:

1. It's not held under excess pressure.
2. It's transmissivity T is not a constant
3. Have storage coefficient (S_Y) greater than 10^{-2}

According to investigation, the geological conditions of the layer of aquifers in city Melhus, Norway fits the case of unconfined aquifers.

4.3 Abstraction well design in unconfined aquifers

A well screen is used to prevent the inhalation of sediment particles in pumping water. However, it's also inevitable to make a trade-off between water yield Z and screening rate. The general equation linking water yield Z to drawdown for a given r (radial distance from well), T (transmissivity), S (storage coefficient) and t (given time) is proposed by Cooper et al. (1967) under an assumption $\frac{r_w{}^2 S}{Tt}$ is less than 0.2 is presented as follows,

$$s = \frac{2.3Z}{4\pi T}\log_{10}\left(\frac{2.25Tt}{r_w{}^2 S}\right)$$

From the equation, conclusions can be drawn that drawdown s increases in proportion to $\log_{10}(t)$ and decreases in proportion to $\log_{10}(r_w)$. From this perspective, it's also suggested to drill to a deeper layer of the aquifer to avoid the case that water level falls below the top of the well screen. As long as it exceeds available drawdown, air is introduced to the system and unwanted side-effects like oxidation and precipitation of iron may arise correspondingly.

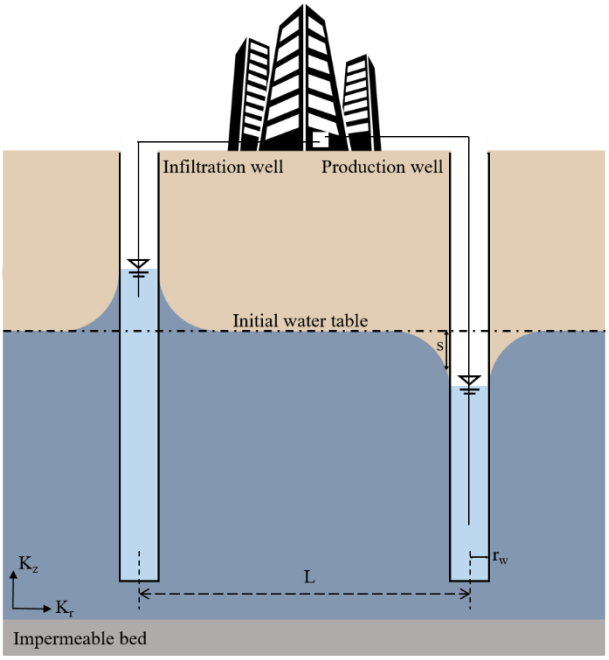

Figure 4: Schematic of unconfined Aquifer (source: Three-dimensional saturated-unsaturated flow with axial symmetry to a partially penetrating well in a compressible unconfined aquifer)

4.4 Hydraulic breakthrough in a well doublet

A well doublet consists of a production well and an injection well. For a rudimentary well doublet where the injection well is located at a distance L down the hydraulic gradient of the aquifer as is shown in figure X, groundwater with a specific volumetric heat capacity S_{VCwat} is pumped out at a certain abstraction rate Z from an aquifer with an initial temperature θ_{gout} and reinjected back to the aquifer at temperature θ_{gin}.

Heat rejected to groundwater (G) is given by:

$$G = (\theta_{ginj} - \theta_{gout}) S_{VCwat} Z$$

Average cooling load (c) with a seasonal performance factor SPF_C for the system is given by:

$$c = (\theta_{ginj} - \theta_{gout}) S_{VCwat} \frac{Z}{(1 + 1/SPF_c)}$$

The production well is normally sited up the hydraulic gradient from the injection well intentionally incase water cooled down (heated) by evaporator migrates with groundwater flow after reinjection and consequently find its way back to the production well. The reentry of the waste water is called a hydraulic feedback in a well doublet. Despite the fact that placing the production well up the hydraulic gradient can partially help with the feedback, risk still exists

in that the natural hydraulic gradient i is generally not large enough to hold up the feedback ($i < i_{rev}$). The expression for a shortest L to trigger the hydraulic feedback under a natural hydraulic gradient i and transmissivity T is given by Clyde and Madabhushi et al. (1983) in *Spacing of wells for heat pumps*.

$$L < \frac{2Z}{T\pi i}$$

For a well doublet placing closer than the critical distance, waste water reinjected is likely to reenter the production well thus leading to a significant decrease (increase) of the temperature of the abstracted water. This will results in a negative influence upon the efficiency and sustainability of the system. To avoid the influence, one might easily draw a misleading conclusion from the equation that we shall place the production well and injection well far enough to avoid the affection. As a matter of fact, it commonly takes hundreds of meters to completely remove the threat of hydraulic breakthrough which is obviously unrealistic in practice. From this perspective, we have to be used to live with the risk of breakthrough yet it does not necessarily indicates a considerable and intolerable effect on efficiency and sustainability for reasons as follows:

1. It usually takes weeks or month for hydraulic feedback to take place. If the heat pump system is put into operation discontinuously, e.g. only put into operation in working hours, the feedback phenomenon will be further postponed.
2. Even if the system is operating all year around, only a small portion of water reinjected will finds its way to the production well.
3. GWHP system has a unique advantage over GCHP system for its wells can be put into reversible operation in heating and cooling mode. This contributes significantly in countervailing the thermal breakthrough in a single working season.

Apart from establish a numerical model for simulation, there are two analytical methods of assessing the hydraulic breakthrough time t_{hyd} for simple dipole systems: Darcy's Law and Double Breakthrough method (Fetter, 2000).

By Darcy's law, Darcy velocity v_D (flow rate per unit cross-sectional area of aquifer) is given by:

$$v_D = Ki_{rev} = \frac{K\Delta h}{L}$$

Where linear velocity of groundwater can be derived by have Darcy velocity v_D divide by effective porosity n_e:

$$v = \frac{v_D}{n_e} = \frac{Ki_{rev}}{n_e} = \frac{K\Delta h}{Ln_e}$$

Therefore, the hydraulic breakthrough time t_{hyd} can be obtained by have the distance between production and reinjection well (the shortest distance water molecules have to travel) divided by linear velocity:

$$t_{hyd} = \frac{L}{V} = \frac{L^2 n_e}{K\Delta h}$$

The method can be further enhanced by employing a Potentiometric surface through which breakthrough time can be divided into a series of sub-items as is shown in figure 5:

$$t_{hyd} = 2 \times \sum_{i=1}^{n} t_i = \frac{2n_e}{K\Delta h} \sum_{i=1}^{n} {L_i}^2$$

As is compared to the undivided equation $t_{hyd} = \frac{L^2 n_e}{K\Delta h}$, the decomposition enhancement considerably stiffens the accuracy of resolving the hydraulic breakthrough time.

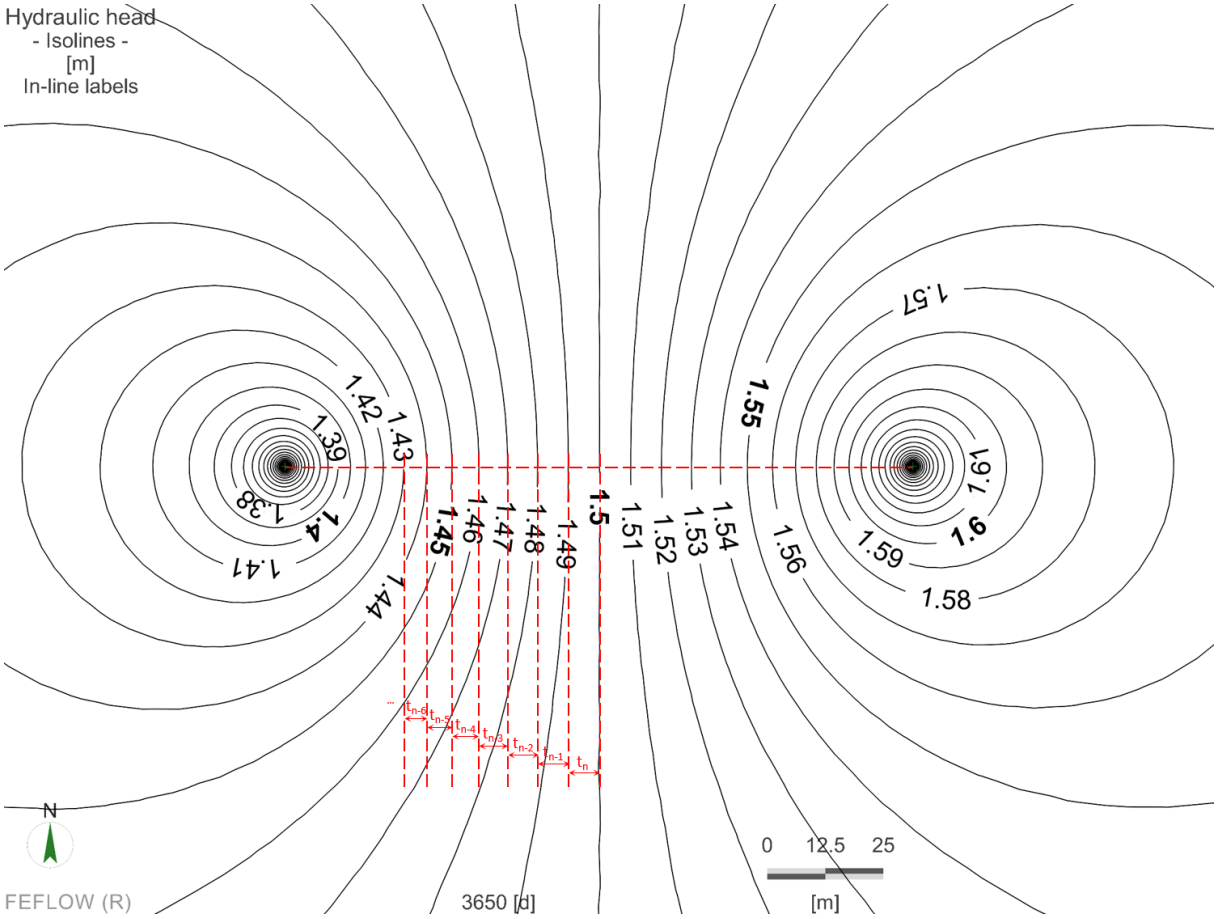

Figure 5: Potentiometric surface to be used in enhancing the accuracy for resolving hydraulic

breakthrough time by Darcy's law

By Double Breakthrough method (Grove and Beetem, 1971), the hydraulic breakthrough time t_{hyd} is given by:

$$\begin{cases} t_{hyd} = \pi n_e D \dfrac{L^2}{3Z} & \text{(if natural hydraulic gradient i is insignificant)} \\ t_{hyd} = \dfrac{Ln_e}{Ki}\left[\dfrac{\beta}{\sqrt{\beta-1}}\tan^{-1}\left(\dfrac{1}{\sqrt{\beta-1}}\right)-1\right] & \text{(if natural hydraulic gradient i is significant)} \end{cases}$$

Where β is an artificial variable equal to 2Z / (TπiL).

Both methods are based on a communal assumption that the migration of both heat and groundwater in the well doublet is confined to a horizontal (2 dimensional) plane. The assumption fits well for most groundwater migration yet it deviates from the actual conditions of heat transfer. Even though both models can be used to track down hydraulic breakthrough time t_{hyd}, they are slightly different from each other in application. Darcy's law is better justified for linear flow where production wells and injection wells are regularly distributed in matrix. Double Breakthrough method, by contrast, accommodates well to irregularly scattered wells where the flow path can be better described in arcs and circles as is shown in Fig 6.

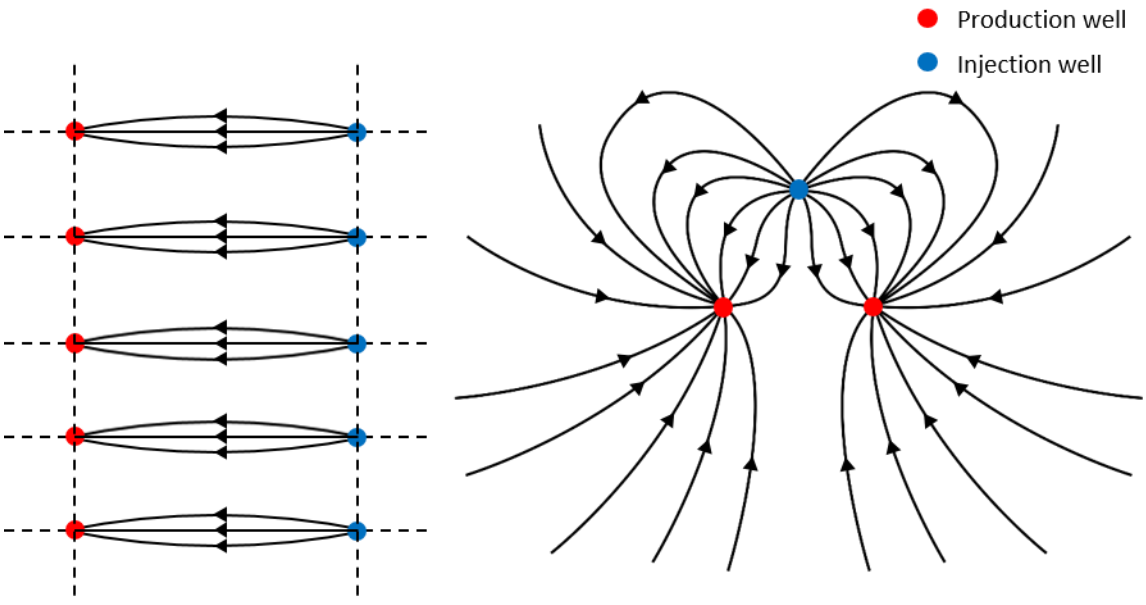

Figure 6: Matrix distribution of wells versus irregularly scattered wells

Apart from hydraulic breakthrough time, the proportion of water recirculated from the injection well to the aggregate groundwater abstraction rate Z (Luo and Kitanidis, 2004) can also be

calculated by:

$$f_{recirc} = 1 - \frac{2}{\pi}(\tan^{-1}\left(\frac{1}{\sqrt{\beta - 1}}\right) + \frac{\sqrt{\beta - 1}}{\beta})$$

Holding other variables as constant, the internal relationships between hydraulic breakthrough time recirculated proportion with the other variable can be intuitively seen as is shown in figure 7,8 and 9.

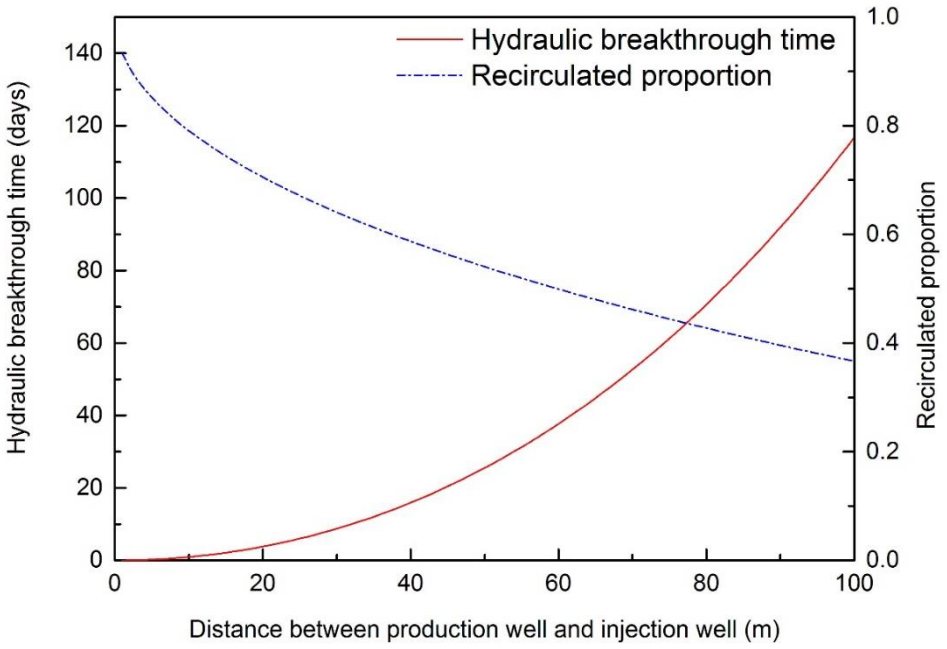

Figure 7: The relation between Hydraulic breakthrough time t_{hyd}, recirculated proportion f_{recirc} and distance between a well doublet L (T=150m^{2}day^{-1}, Z=10Ls^{-1}, D=75m, K=T/D=2mday^{-1}, ne=0.1, i=0.01)

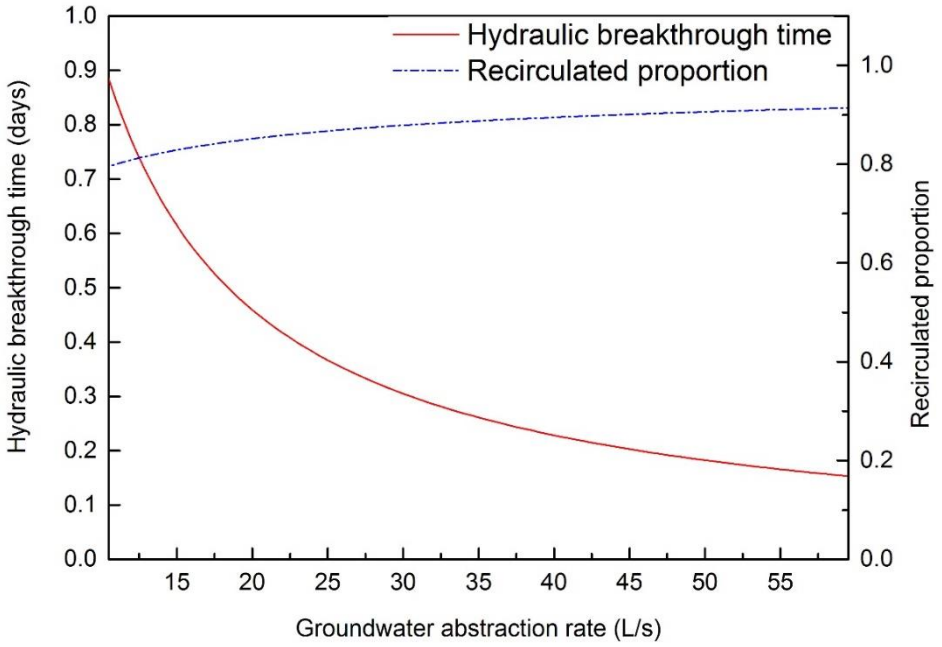

Figure 8: The relation between Hydraulic breakthrough time t_{hyd}, recirculated proportion f_{recirc} and the groundwater abstraction rate Z (L=10m, Z=10Ls^{-1}, D=75m, K=T/D=2mday^{-1}, ne=0.1, i=0.01)

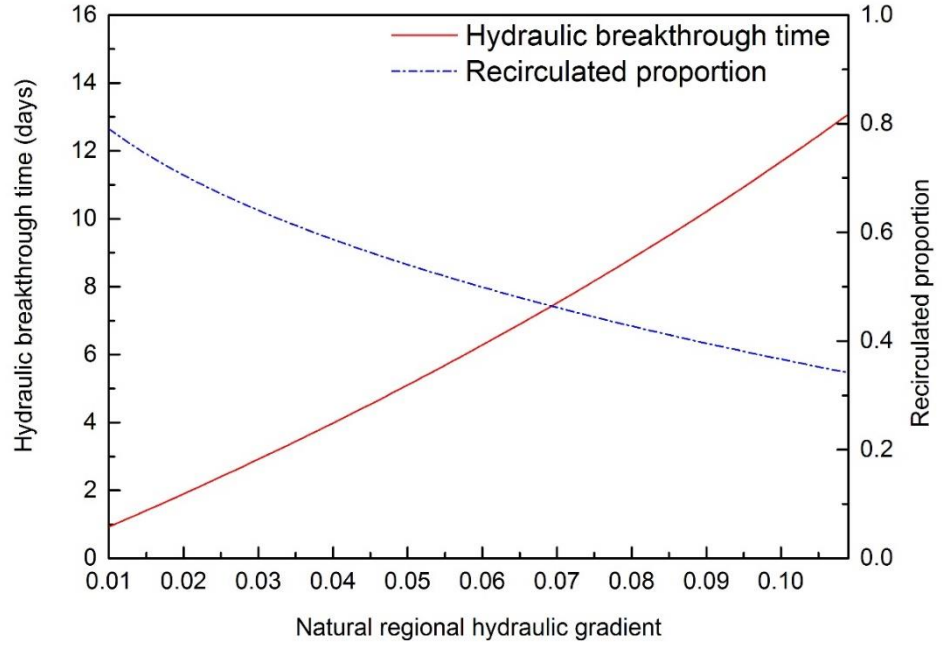

Figure 9: The relation between Hydraulic breakthrough time t_{hyd}, recirculated proportion f_{recirc} and natural regional hydraulic gradient i between a well doublet L (L=10m, T=150m^{2}day^{-1},

Z=10Ls^{-1}, D=75m, K=T/D=2mday^{-1}, ne=0.1)

Figure 7 reveals the fact that the hydraulic breakthrough time increases with an increasing distance between the well doublets whereas the recirculated proportion drops dramatically at the meantime. Besides, Figure 8 presents that the upsurge of groundwater abstraction rate also contributes to a significant decrease in hydraulic breakthrough time. Apart from all these, the natural regional hydraulic gradient also plays a critical role in affecting the hydraulic breakthrough time and recirculated proportion. In figure 9 the hydraulic breakthrough time t_{hyd} is roughly in proportion to hydraulic gradient i and the recirculate proportion f_{recirc} is roughly inversely proportional to hydraulic gradient i.

Since the abstraction rate is largely determined by the design heating (cooling) load and pumping equipment, we have to resort to other means to extend the breakthrough time and reduce the recirculation proportion. These approaches include (1) Have the production well and injection well sited away from each other as long as there is sufficient space. (2) Drill the wells at which the natural regional gradient is relatively high. (3) Arranged production well and injection well in line with a direction normal to potentiometric contour.

4.5 Thermal breakthrough in a well doublet

Under the assumption of instantaneous thermal equilibration, the mathematical equation for describing heat transferred in ground water environment is given by Marsily (1986) in his *Quantitative hydrogeology*:

$$\lambda_{\mathrm{eff}}\frac{\mathrm{d}^2\theta}{\mathrm{dx}^2}-\mathrm{S_{VCwat}}\frac{\mathrm{d}(\mathrm{V_D}\theta)}{\mathrm{dx}}=\mathrm{S_{VCaq}}\frac{\mathrm{d}\theta}{\mathrm{dt}}$$

Where λ_{eff} stands for the effective thermal conductivity of the saturated aquifer, v_D for Darcy velocity, θ for transient temperature, t for given time, S_{VCwat} and S_{VCaq} for the volumetric heat capacities of the groundwater and the saturated aquifer respectively ($S=\rho C$).

The equation is a combination of heat transfer by conduction presented in the first term, convection in the second term and the changing rate of the heat preserved in a unit volume of aquifer.

Under an additional presumption of two dimensional heat transfer (as is mentioned in former chapter, the assumption confines the heat within the aquifer and deserves elaboration), the

thermal breakthrough time t_{the} is given by

$$\begin{cases} t_{the} = \pi D \dfrac{S_{VCaq} L^2}{3 S_{VCwat} Z} & \text{(if natural hydraulic gradient i is insignificant)} \\ t_{the} = \dfrac{L S_{VCaq}}{S_{VCwat} Ki} \left[\dfrac{\beta}{\sqrt{\beta - 1}} \tan^{-1} \left(\dfrac{1}{\sqrt{\beta - 1}} \right) \right] & \text{(if natural hydraulic gradient i is significant)} \end{cases}$$

Compare the expression for both t_{hyd} and t_{the}, it's clear that they are in proportion to each other with a slope coefficient termed thermal retardation R_{the}. Since heat transfer is significantly slower than groundwater, the thermal retardation R_{the} defined by the ratio between thermal and hydraulic breakthrough time is normally greater than 1. In *Spacing of wells for heat pumps* Clyde and Madabhushi (1983) also includes an empirical equation (also restricted by the presumption of two dimensional heat transfer) to predict the temperature of the abstracted water θ_{gout} after breakthrough:

$$\frac{\theta_{gout} - \theta_{ginj}}{\theta_0 - \theta_{ginj}} = 0.34 \exp\left(-0.0023 \frac{t}{t_{the}}\right) + 0.34 \exp\left(-0.109 \frac{t}{t_{the}}\right) + 1.37 \exp(-1.33 \frac{t}{t_{the}})$$

Where θ_{ginj} stands for the temperature of injected water and θ_0 for initial groundwater temperature.

If three dimensional heat transfer is taken into consideration where heat might disperse into contiguous aquitard, the thermal breakthrough time t_{the} is significantly underestimated. The underestimation can be even more serious if the aquifer is too close to ground surface. As is presented in figure 11 and 12, the underground temperature has a close interaction with the changing air temperature at shallow layers (less than 10m) where the heat accumulation will be further impaired by vertical heat transfer with ambient air above ground.

To figure out the depth above which ground temperature is significantly influenced by changing air temperature, a one-hundred-meter depth model is established by FLUENT (a widely used CFD software) as is shown in figure 10. At the top layer of the model, udf series were implemented with data acquired from weather website (worldweather.cn, 2016) shown in Table 2 and 3.

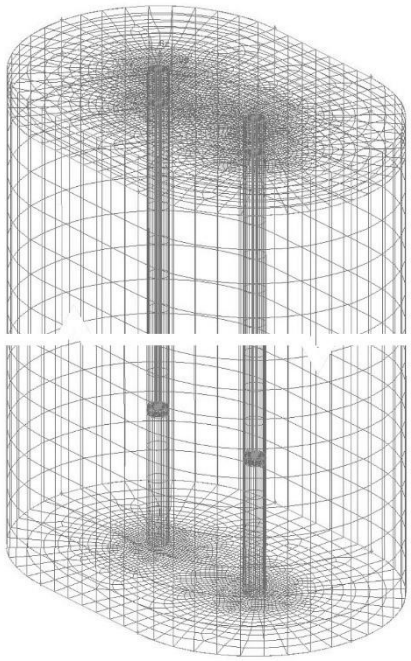

Figure 10: Fluent model to test the influence depth of changing air temperature

Table 2: Temperature of Shanghai measured by months (Source: worldweather.cn)

Shanghai	Jan	Feb	Mar	Apr	May	Jun	Jul	Aug	Sep	Oct	Nov	Dec
Daily maximum temperature	7.6	8.7	12.6	18.5	23.2	27.8	31.8	31.6	27.4	22.4	16.8	10.7
Daily minimum temperature	0.3	1.1	4.9	10.4	15.3	20.1	24.7	24.7	20.5	14.3	8.6	2.7

Table 3: Temperature of Trondheim measured by months (Source: worldweather.cn)

Trondheim	Jan	Feb	Mar	Apr	May	Jun	Jul	Aug	Sep	Oct	Nov	Dec
Daily maximum temperature	-2	-2	0	3	8	12	15	14	9	5	1	-1
Daily minimum temperature	-6	-6	-5	-2	2	6	9	8	4	1	-3	-5

Simulation results imply that temperature series at a depth of 2 meters fluctuates violently according to the change of surface air temperature. In comparison, temperature series at a depth of 5 meters have a moderate fluctuation yet with a more significant lag in phase. However,

temperature series at a depth of 10 meters, no matter Shanghai or Trondheim, reveals little deviation from its constant value. This proves that influence of surface air temperature is confined to shallow layers of ground no deeper than 10 meters. Besides, heat accumulated under 10 meters can hardly be affected by changing surface air temperature. From this perspective, we can selectively neglect the influence of surface air temperature as long as filter is more than 10 meters beneath ground surface.

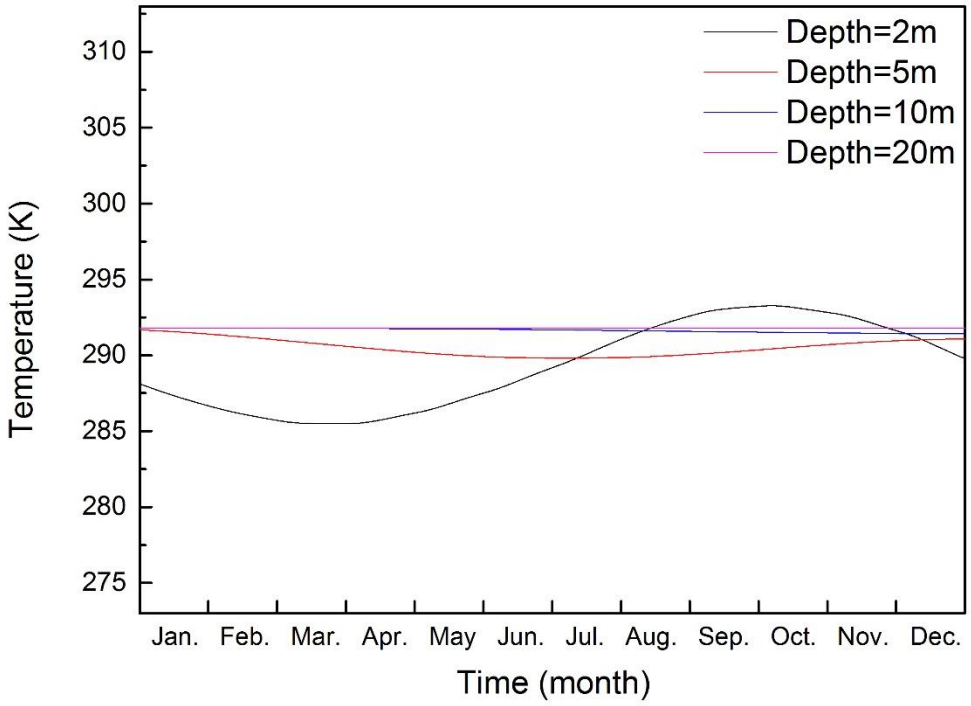

Figure 11: Underground temperature change in Shanghai at different depth in 2015 according to Fluent model simulation

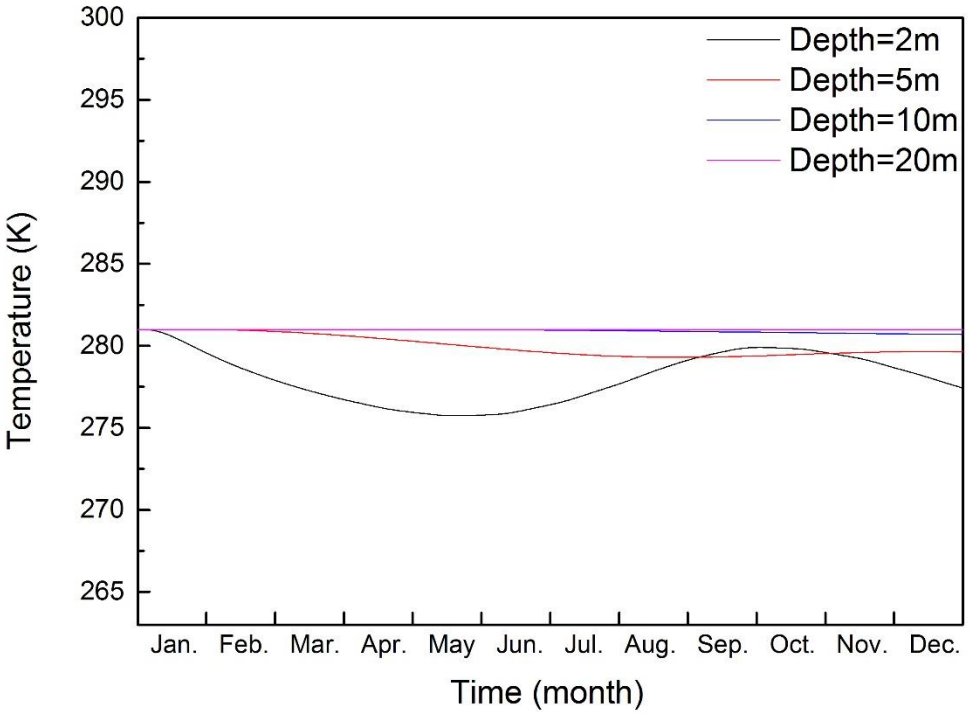

Figure 12: Underground temperature change in Trondheim at different depth in 2015 according to Fluent model simulation

5. Research background for heat transfer Modelling

To help control the overall performance and improve the efficiency and sustainability of the heat pump system, models are established therefore being able to predict the thermal response under different design parameters and groundwater flow conditions. These models fall into two categories: analytic models and numerical models.

5.1 Analytic models

Known as the most critical component of the GSHP system, various versions of analytic models for BHEs have been proposed to simulate its heat transfer process, including ILS, ICS, FLS model. Despite the fact that these models were all designed for vertical closed systems, similar conclusions are drawn that groundwater flow helps enhance heat transfer between BHEs and its surrounding environment.

5.1.1 Infinite line source model

The infinite line source model (ILS) proposed by Ingersoll et al. (1948) is the earliest approach of BHEs simulation. The infinite line source model does not account for the length of the borehole. The point is, the underlying presumption for ILS model is that the line source can be represented by an in series of point sources. Simple as it is, the solution of ILS model is limited by mainly two factors:

1. The entire borehole is simplified to a point source, therefore the borehole is presumed to have the same thermal properties of the surrounding soil. The premise leads to a huge difference in treating heat conductivity especially when the boreholes is refilled with grout while the surrounding soil is soaked in groundwater. As a result, IFS model is not appropriate for simulating early transients (Yang et al., 2010).
2. ILS model neglects the axial heat transfer which is proved to be essential by Marcotte et al. (2010), Zeng et al. (2002) and Molina-Giraldo et al. (2011). From this perspective, infinite line source model is not suitable for long-term simulation where the axial heat transfer shall be reflected.

5.1.2 Infinite cylindrical model

Likewise the ILS model, Infinite cylindrical solution proposed by Jaeger (1956) presents a solution in an infinite medium bounded internally by a cylindrical surface. The Infinite cylindrical model (ICS) is evolved from the Infinite line source model and therefore carries on the common limitation of neglecting the thermal capacity within the borehole and not being able to reflect the axial heat transfer. Hence the solution is also not favorable for early transients and at long timescales.

5.1.3 Finite line source model

In comparison to the ILS model and ICS model, the finite line source model (FLS) accounts for the finite length of the borehole and the heat transfer along the axial dimension (Eskilson, 1987). Therefore, it provides more accurate solution at long timescales. Even though it inherits part of the disadvantages of the Infinite line source model and still not accurate for early transients, the finite line source model is considered the most appropriate analytic solution for BHEs.

5.2 Numerical models

Compared to analytical models, numerical models generally has a higher accuracy and can be better customized according to real scenarios. More importantly, numerical models allow a deeper investigation into influence exerted on system efficiency by groundwater characteristic and other external factors.

Normally, a typical computational fluid dynamics (CFD) software called Fluent could be used to simulate the transient performance of Ground source heat pumps. Fluent includes well-validated physical modeling capabilities to deliver fast, accurate results across the widest range of CFD and multi physics applications. By establishing a model in Fluent, it helps users in predicting and controlling the dynamic performance under fluid flow in optimizing the efficiency of products and processes. Hence, users can have the confidence that the product will perform optimally before the prototype is made or the project goes into execution.

However, as is the same with the analytical models mentioned above, Fluent is more suitable an instrument for dealing with closed systems that employ one or more pipes or borehole heat exchangers where heat preserved beneath the ground is mined through a segregate heat carrier

fluid in BHE. In contrast, open systems, as is the case in Melhus, operate with groundwater abstraction and injection wells where groundwater is directly brought to the surface would have to seek other means of simulation.

Professional software are apparently more appropriate alternatives for investigating the complex heat transfer process on a grand scale. Jozsef et al. (2010) offers a comprehensive list of models that have been used or are potentially suitable for both convective and conductive heat transport simulations of shallow GSHP systems as is presented in table 4. Among all these methods, Feflow modelling is broadly applied to solve mass and heat subsurface problems. A major advantage of utilizing Feflow is that it is fully coupled thus allowing handling temperature dependencies of density and viscosity. Unlike AQUA3D mainly designed for simulating mass-transport problems (Wei and Ende, 2004) rather than heat transfer and SUTRA specialized in two-dimensional simulation for subsurface environment, FEFLOW generates a three-dimensional finite-element method for simulating both mass and heat transport (Deng Z., 2004) in density-dependent groundwater system.

Table 4: Numerical Codes Suitable for Heat Transport Simulations of Shallow Geothermal Systems Considering Groundwater Flow (Jozsef et al. 2010)

Code name	Method	Process	Process[1]	Availability	Comments	Reference
AST/TWOW[2]	FD	H, T	H→T	Commercial	3D, calculates near-field heat transport around BHEs	Schmidt and Hellström (2005)
BASIN2	FD	H, T, C	H↔T, M, CH	Free code	2D, simulates sedimentary basin development. Cross-sectional view	Bethke et al. (2007)
COMSOL[2]	FE	H, T, C	H↔T	Commercial	3D, multi-physics (more processes can be coupled)	Holzbecher and Kohfahl (2008)
FEFLOW[2]	FE	H, T, C	H↔T, M, C	Commercial	2D, 3D	Diersch (2002)
FRACHEM	FE	H, T, C	H↔T, M, C	Scientific	3D, used for Hot Dry Rock modeling	Bächler (2003)
FRACture[2]	FE	H, T	H↔T, M	Scientific	3D, developed for Hot Dry Rock modeling	Kohl and Hopkirk (1995)
ROCKFLOW /GeoSys	FE	H, T, C	H↔T, C	Scientific	3D, fracture systems can be included. Allows for multi-phase flow	Kolditz et al. (2001)

HEATFLOW[2]	FE	H, T	H↔T	Free code	1D, 2D, 3D	Molson and Frind (2002)
HST2D/3D	FD	H, T, C	H↔T, M, CH	Free code	2D, 3D	Kipp (1986)
HydroTherm	FD	H, T	H↔T	Free code	2D, 3D, two-phase model. Can simulate 0 to 1200 °C	Kipp et al. (2008)
HYDRUS-2D	FE	H, T, C	H→T	Commercial	2D, unsaturated zone, plant water uptake is considered	Šimùnek et al. (1999)
SEAWAT	FD	H, T, C	H↔T, C	Free code	3D	Langevin et al. (2008)
SHEMAT[2]	FD	H, T, C	H↔T, C	Commercial	3D	Clauser (2003)
SUTRA	FE/FD	H, T, C	H↔T, C	Free code	2D, 3D	Voss and Provost (2002)
THETA[2]	FD	H, T, C	H↔T, CH	Scientific	3D	Kangas (1996)
TOUGH2	FD	H, T, C	H↔T, C, CH	Commercial	1D, 2D, and 3D. Allows for multi-phase flow	Pruess et al. (1996)
TRADIKON 3D[2]	FD	H, T	H→T	Free code	3D, specially designed for BHEs assessments	Brehm (1989)
VS2DH	FD	H, T	H→T	Free code	2D	Healy and Ronan (1996)

Note: H, Hydraulic; T, Temperature; C, Contaminant (solute).
1H→T, fluid flow is independent of T; H ↔ T, fluid flow depends on T; M, mechanical deformation (pore deformation); CH, chemical reaction.
2Already used for GSHP simulations.

Given the software of Feflow, approaches for assessing the sustainability of a regional area for BHEs installation differ. Fujii et al. (2007) elaborates the minimal heat storage operation required for long-term application (up to 50 years) of GCHP systems. The model was used to investigate different operational schemes and sustainability is predicted and compared in form of heat extraction rate. Despite the fact that such method is only applicable for closed-loop system, a slight change in replacing the heat extraction rate with regional temperature contour and abstraction temperature can solve the problem. Russo et al. (2009) focus on figuring out the most appropriate configuration (i.e. the location and pumping rates) for ensuring the regional sustainability GWHP systems. The simulation is performed assuming steady-state conditions for groundwater flow and transient conditions for heat transport (in case of heat dispersion as is mentioned in Chapter 2.5). However Russo only considered a 120 days cooling operation per year, presuming “ground water system can be expected to recover thermally

between annual cycles". Yet such assumption will inevitably leads to an overestimation in allowable abstraction rate and the impact on aquifers in terms of Potentiometric surface. Other articles of Russo (2012) concentrates on early evaluation of thermally affected zone (TAZ) around the infiltration well. The article adopted a two-layer model yet failed to take vertical heat flux across aquifer boundary into consideration thus overestimate the calculated thermal plumes.

In the model to be established, we'll lay attention on regional heat transfer between abstraction and infiltration wells and factors affecting the extent of unwanted interactions. The simulation time is designed to last for 10 years since one-year simulation is apparently not enough to account for the thermal influence accumulated and 50-year simulation is far beyond the service life of the systems. Finally, feasible solutions will be given to delay the adverse impact brought by the interaction.

6. Site description

6.1 General description

Melhus, 175 meters above sea level, locates in the river valley of Gauldalen, 2 miles south of Trondheim, with an area of about 692km2 and 15000 residents. River Gaula flows through the city center from south to north and runs into the Trondheim fjord. The survey area is located is highlighted in figure 13.

According to data collected at weather station Løksmyr in Melhus (2015), the average annual precipitation in Melhus is around 700-1000mm/year; the average temperature of Melhus is 5-6 degrees Celsius.

Melhus's landscape is largely shaped by the last ice age and is an area with considerable sediment deposits as is shown in figure 14. The surface of the city center is mostly thick clay with alternating layers of sand, silt, fine sand and gravel deposits while the surface outside is primarily covered by alluvial deposits. On the north side of Melhus center lies a significant soil ridge called Melhus back. Melhus back is 120 meters above sea level at its highest, and is mainly consists of a 10 to 30 meter thick layer of clay and silt-overarching masses.

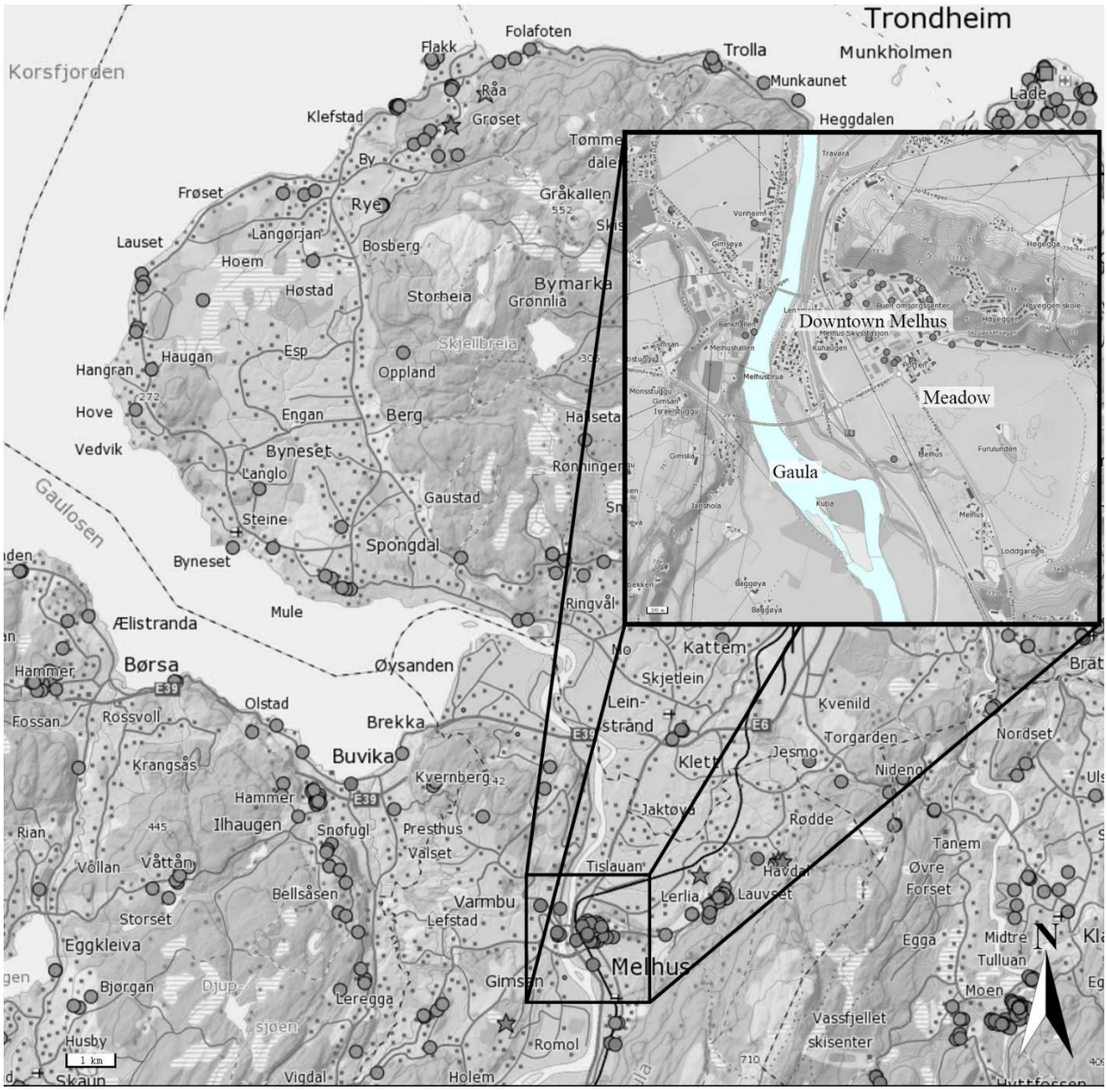

Figure 13: Map of city Melhus in Trondheim area (Source: NGU database)

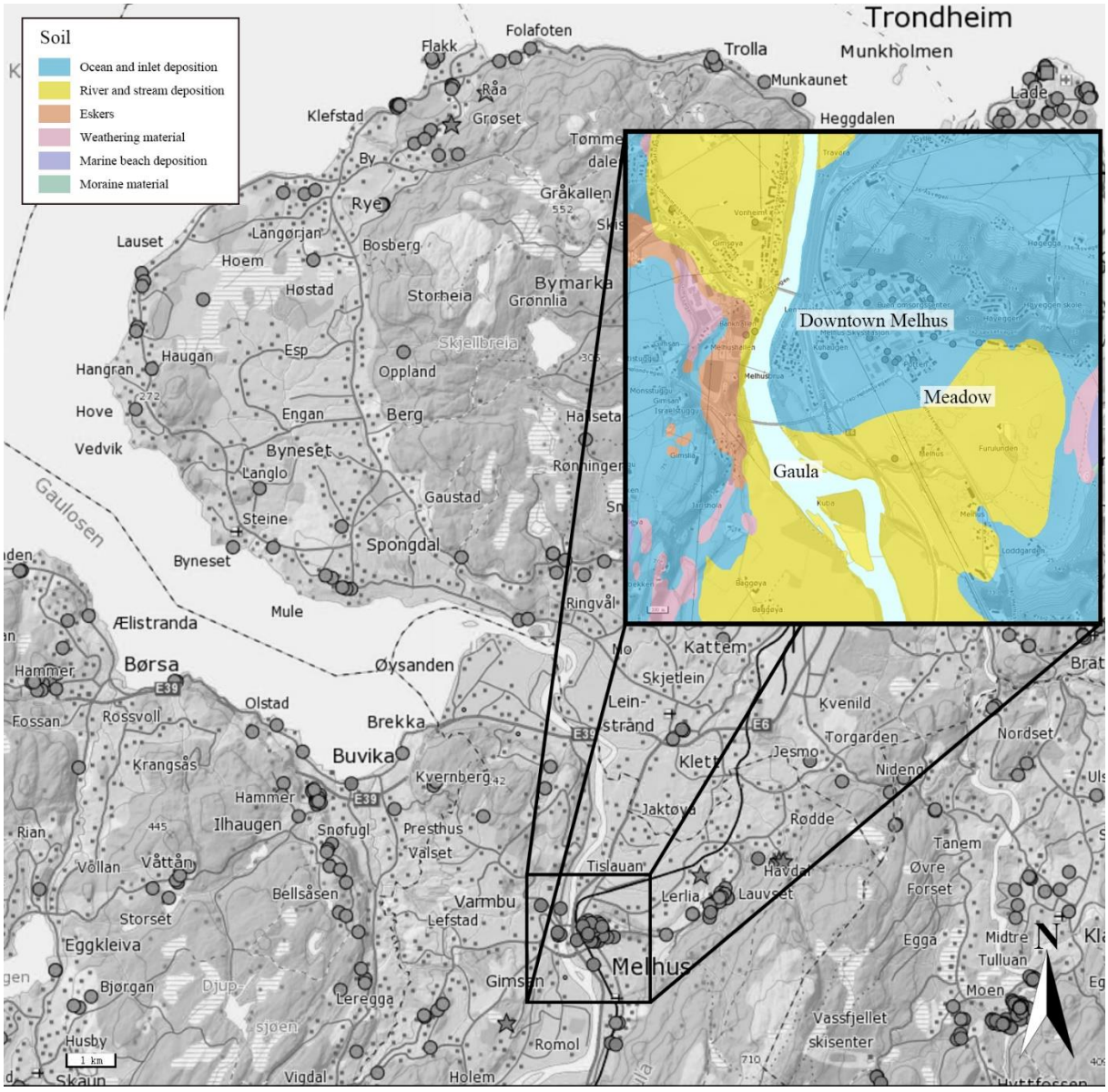

Figure 14: Soil component map of city Melhus (Source: NGU database)

There are 25 existing wells in Melhus the majority of which are locate to the east of river Gaula. These wells are either used as production wells or corresponding infiltration (injection) wells, except some individual production wells which directly drain into the stormwater drainage system. As is presented in figure 15, the production wells are highlighted in red, infiltration wells in blue. Apart from the existing wells, new wells are drilled and presented in green. These wells have not been put into operation and can switch between production wells and infiltration wells according to the long-term suitability.

The two adjacent new wells to be investigated in the report locate near Melhus' fire station and is demarcated in figure 15 with a cross at the center. Given data provided by NGU database, the wells are find to be 135 meters away from each other. Model based on the two wells would be established accordingly and necessary geological parameters would be discussed in detail in following sections.

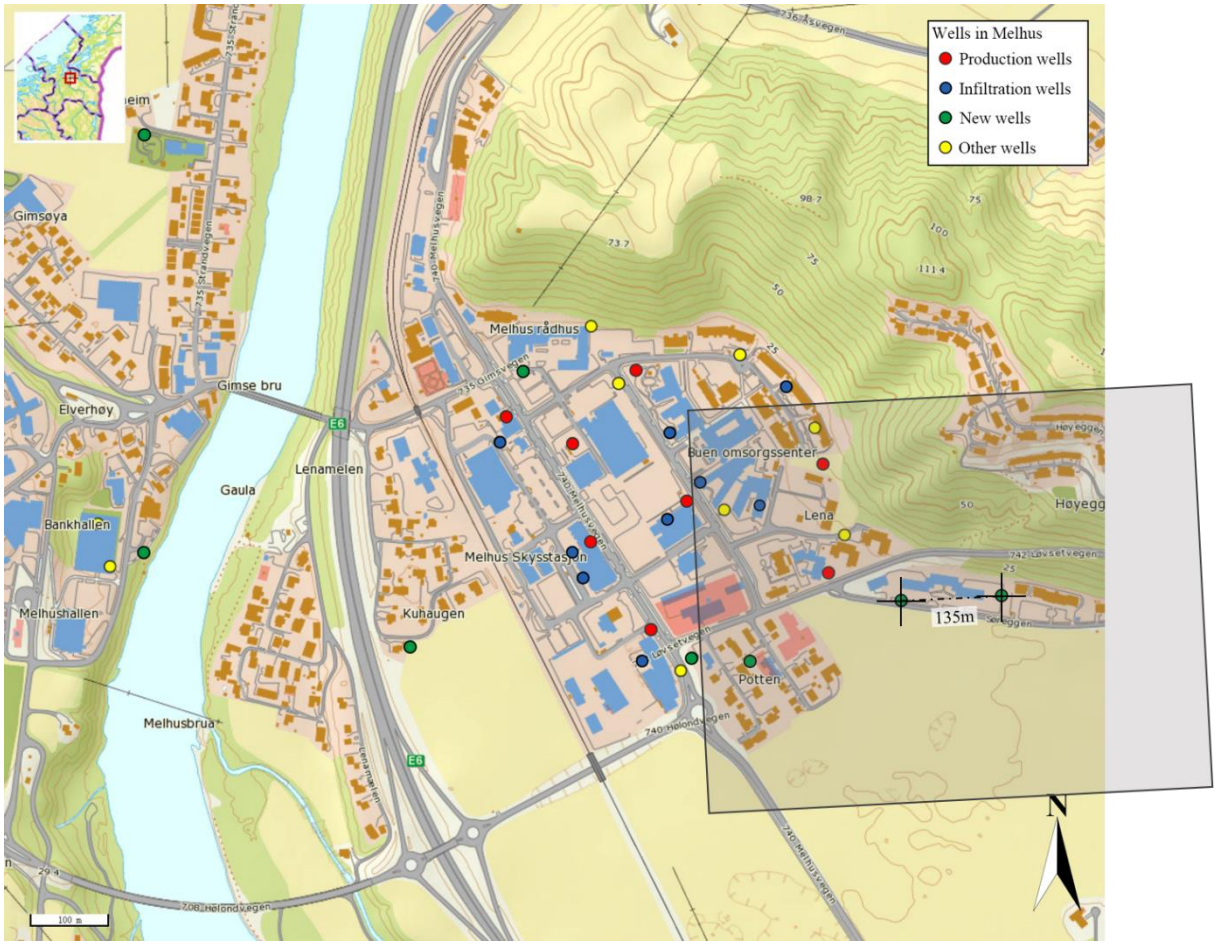

Figure 15: Wells distribution in Melhus center (Source: NGU database)

Figure 16: Well at fire station in Melhus (Source: NGU database)

6.2 Hydro geology

6.2.1 Geological stratification

Samples collected from observation holes at the site tells the strata structure near the fire station as is presented in figure 17. It is composed of layers of geo materials with disparate physical and thermal properties stacking on each other. To make a simplification for modelling, the strata can be generally divided into five layers according to the predominating constituent of each layer, i.e. silt, clay, sandy gravel, gravel and gravelly sand from top to bottom. Production and infiltration wells are drilled to 55m from ground surface (elevation: -39.5) where hydraulic as well as thermal conductivity yields the best.

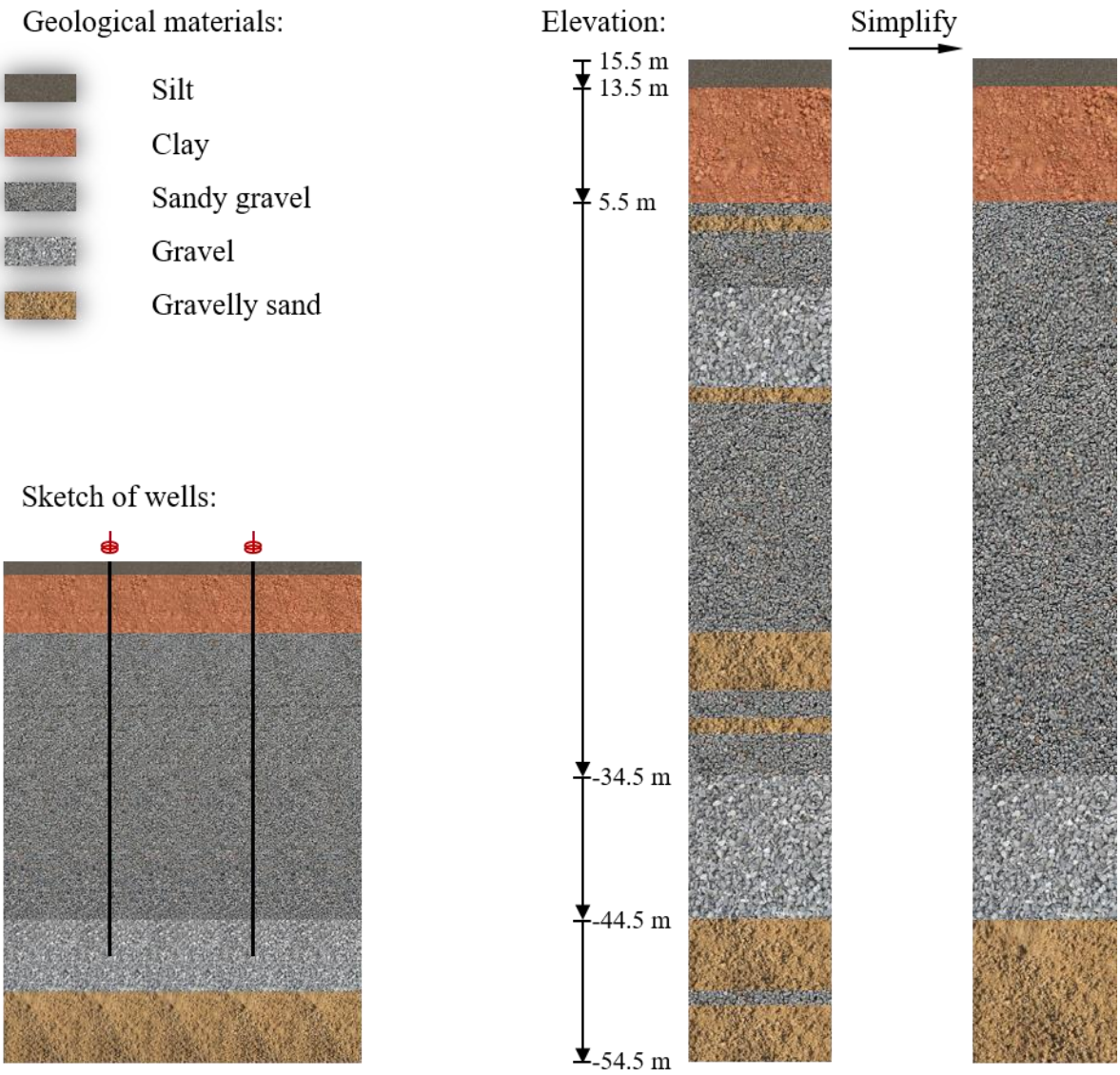

Figure 17: strata structure at the fire station in Melhus

6.2.2 Groundwater flow stratification

Apart from strata structure, experiment at the site tells the distribution of groundwater which can be roughly categorize as six different levels from non-existing to excellent. The distribution of groundwater can be largely classified as a non-existing / existing binary circumstance for modelling where the groundwater speed is simplified as constant while a positive direction is designated to be from west to east locally.

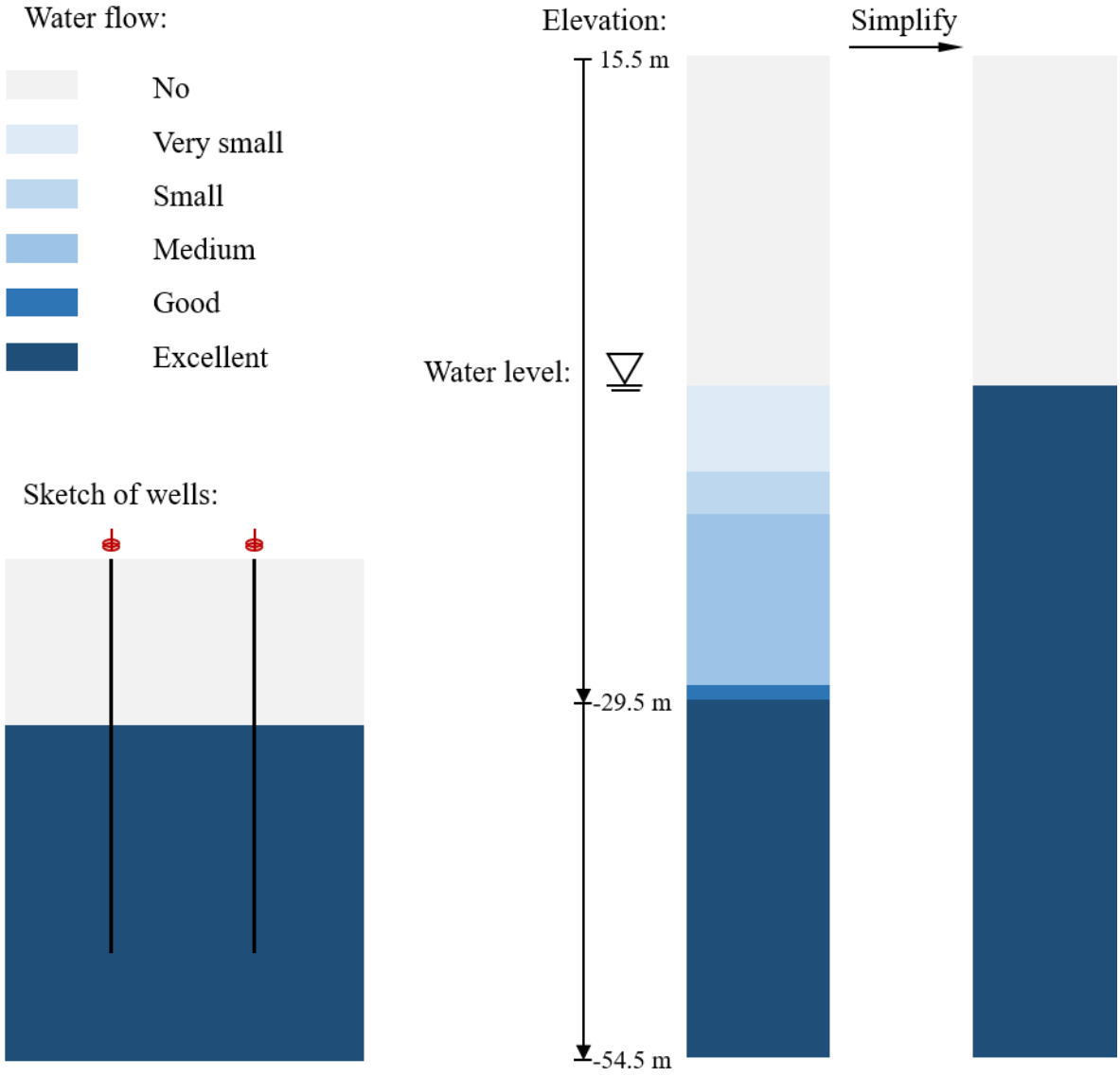

Figure 18: groundwater distribution at the fire station in Melhus

6.2.3 Hydraulic parameters

The effective porosity is considered the porosity available to contribute to fluid flow through the rock or sediment while hydraulic conductivity describes the ease with which a fluid can move through pore spaces or fractures. Porosity values adopted in modelling are presented in Table 5 provided by Brattli (2009) and horizontal hydraulic conductivity is measured through multiple monitors at site as is revealed in table 6.

Table 5: Porosity values adopted in modelling (source: Fysisk og kjemisk hydrogeology)

	Effective porosity (%)
Silt	10
Clay	5
Sandy gravel	35
Gravel	30
Gravelly sand	30

Table 6: hydraulic conductivity adopted in modelling (source: monitors at site)

Monitor depth (m)	Local hydraulic conductivity (m/s)	Monitor depth (m)	Local hydraulic conductivity (m/s)	Monitor depth (m)	Local hydraulic conductivity (m/s)
12	3.31e-5	41	1.68e-3	57	1.37e-2
15	1.74e-4	42	1.16e-3	59	1.63e-3
18	2.31e-2	44	2.23e-4	60	1.63e-3
21	2.18e-3	45	4.84e-4	62	1.61e-3
24	6.69e-4	47	8.18e-4	63	1.17e-3
27	2.40e-3	48	1.06e-3	65	4.86e-4
30	1.49e-4	50	6.91e-4	66	2.68e-3
33	6.07e-4	51	1.15e-3	67	6.70e-4
36	9.04e-4	53	9.62e-4	68	4.00e-4
38	5.74e-4	54	2.97e-3		
39	1.43e-3	56	4.63e-3		

Interval-weight average value of the data collected from the monitors are adopted as horizontal

hydraulic conductivity values of each layer and vertical hydraulic conductivity is postulated an order magnitude smaller compared to corresponding horizontal ones.

Specific heat capacity is the quantity of heat required to raise the temperature of a unit mass by a unit change in temperature while the volumetric heat capacity is calculated by multiplying specific heat capacity by material density. Thermal conductivity is the quantity of heat flows through a unit area under a unit temperature gradient in a unit time.

Typical volumetric heat capacity and thermal conductivity of soil and rocks is given in Table 7 by Williams (1973).

Table 7: hydraulic parameters adopted in modelling (source: Determination of heat capacities of freezing soils)

	Volumetric heat capacity $MJ/m^3 \cdot K$	Thermal conductivity W/(m·K)
Silt	2.5	1.4
Clay	2.2	0.9
Sandy gravel	2.2	3.1
Gravel	2.2	2.04
Gravelly sand	2.5	1.6

7. Model development

7.1 numerical method

Finite volume method is used to discretize the integral form of the convection-diffusion temperature equation (He, 2011):

$$\frac{\partial}{\partial t}\int_V \rho C_p \theta dV + \int_s \rho C_p \theta v n ds = \int_s \lambda \nabla \theta n ds$$

Where n stands for surface normal vector, v for surface velocity vector, $\nabla\theta$ for temperature gradient at cell surface using cell centroid values.

The advection flux term in discrete form is in terms the sum of the convention fluxes through each call face such that,

$$\int_s \rho C_p \theta v n ds = \sum F_i$$

Where F_i stands for all six faces of a hexahedral cell.

7.2 Iterative method

Feflow has two common solver for iteration. BiCGSTABP solver is the defaulted solver for strongly convective problems, yet such solver could generate significant jagged fluctuation in solving thermal problems. Hence, PARDISO solver is adopted in simulation.

7.3 Boundary conditions

Boundary conditions adopted in modeling includes:

All nodes employs a same initial temperature and hydraulic head:

$$\begin{cases} \theta_0 = 7.5℃ \\ h_0 = 1.5m \end{cases}$$

Groundwater abstraction rate:

$$Z = 1296 m^3/d$$

Water Injection temperature:

$$\theta_{in} = 5℃$$

Fluid flux:

$$v = 5 \cdot 10^{-8} m/s$$

8. Modelling methodology validation

To verify whether the methodology adopted of establishing the model is reliable, a validation model wielding to the same methodology is specially built according to experimental data collected from the 23th well at Melhus fire station. Geometric parameters along with boundary conditions adopted in the validation model are listed as follows,

Diameter of the well:

$$\mathrm{d} = 0.168\mathrm{m}$$

Storage coefficient S is presumed to be 0.08.

All nodes employs a same initial temperature and hydraulic head:

$$\begin{cases} \theta_0 = 7.45℃ \\ \mathrm{h}_0 = 3.115\mathrm{m} \end{cases}$$

Groundwater abstraction rate:

$$\mathrm{Z} = 1296\mathrm{m}^3/\mathrm{d}$$

Fluid flux are presumed to be stationary:

$$\mathrm{v} = 0\mathrm{m}/\mathrm{s}$$

Therefore, data is collected at an interval of 0.01 day till the end of the second day thus forming a simulation predicted reference data set.

On the other hand, theoretical drawdown follows the equation derived by Cooper and Jacob (1946) as long as $\frac{\mathrm{r}^2 S}{4\mathrm{Tt}}$ is small in which case higher terms of the polynomial expansion is negligible:

$$\mathrm{s} = \frac{2.3\mathrm{Z}}{4\pi\mathrm{T}}\log(\frac{2.25\mathrm{Tt}}{\mathrm{r}^2\mathrm{S}})$$

Compared to the real time data collected from the site, diagram is produced as is demonstrated in figure Y. Given the fluctuating characteristic of the measured data, a linear regression is performed where we have the intercept equals to 0.10035 and slope equals to 0.0036.

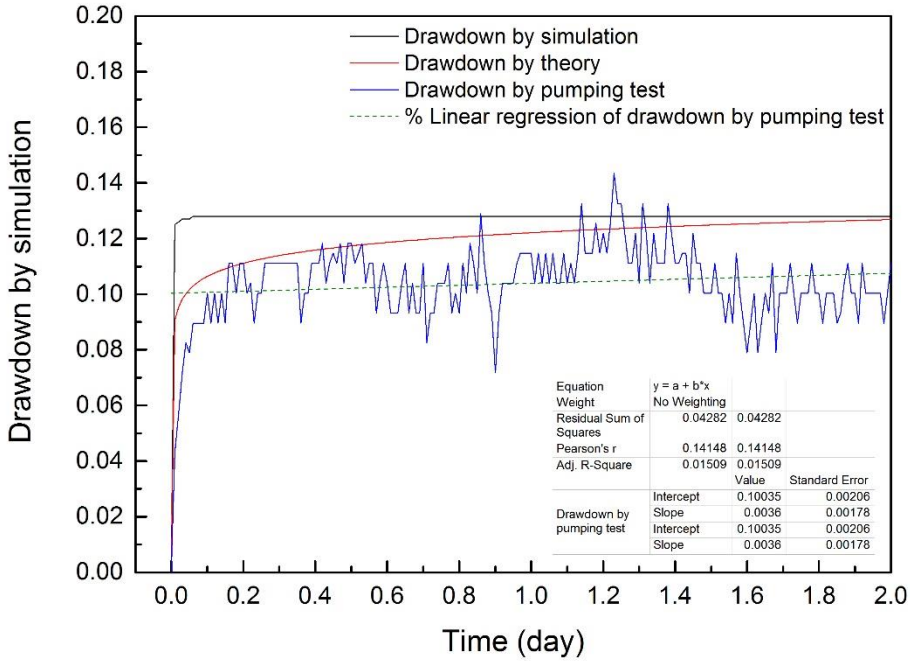

Figure 19: A comparison of drawdown predicted by simulation, theory and measured.

At the end of second day, we have drawdown predicted by simulation equals to 0.128m. Meanwhile, the theoretical drawdown given by Cooper's equation equals to 0.12684m and the linear regressed value given by measured data equals to 0.10755m. Having theoretical data set as a benchmark, the error of simulation results and measured results are 0.9145% and 15.21% respectively.

The results implies that the reliability of the results predicted by simulation and the possible explanation for the remaining error could be:

1. Systematic inaccuracy in pumping test.
2. Groundwater flow is not stationary
3. Storage coefficient deviates from the presumed value of 0.08
4. The Affection by precipitation and the ever rising Gaula river.

The last point, i.e. precipitation and the influence by level of the river have such a significant influence upon measured data that the long-term drawdown data measured have little capability.

9. Results

To look into the influence of the relative direction of groundwater flow, an abstraction well is designed to situate up, on the same and down the hydraulic gradient from an infiltration well respectively as is presented in figure 20. Besides, observation points are set at outlet of abstraction points and 5 meters above and below the points.

Multiple external factors were tested for their individual influence on breakthrough time and a comprehensive diagram is presented to illustrate their influence on the system's long-term efficiency.

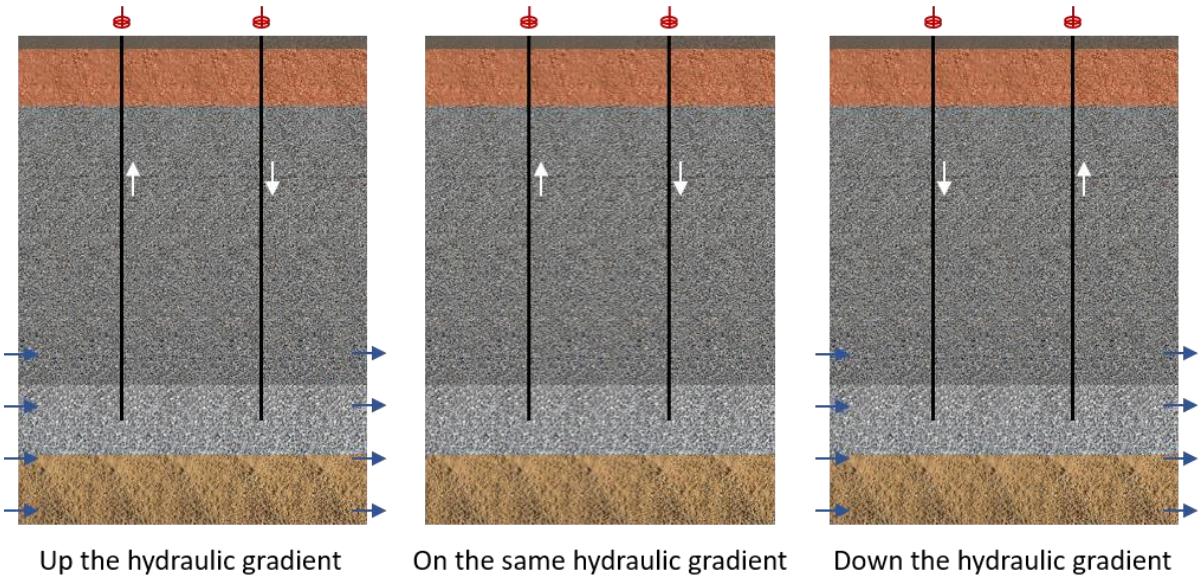

Figure 20: schematic diagram for different relative direction of groundwater flow

9.1 Hydraulic breakthrough time

There are two different means for deriving the hydraulic breakthrough time t_{hyd}. The first and most common method is resorting to a built-in module in Feflow i.e. Trace in module streamlines. The other method evolves both a steady state potentiometric surface diagram and enhanced Darcy's law as has been discussed in chapter 4.4, i.e.

$$t_{hyd} = 2 \times \sum_{i=1}^{n} t_i = \frac{2n_e}{K\Delta h} \sum_{i=1}^{n} {L_i}^2$$

Where n_e stands for effective porosity, K for hydraulic conductivity, Δh for hydraulic head difference between adjacent potentiometric lines and L_i for the shortest distance between adjacent potentiometric lines.

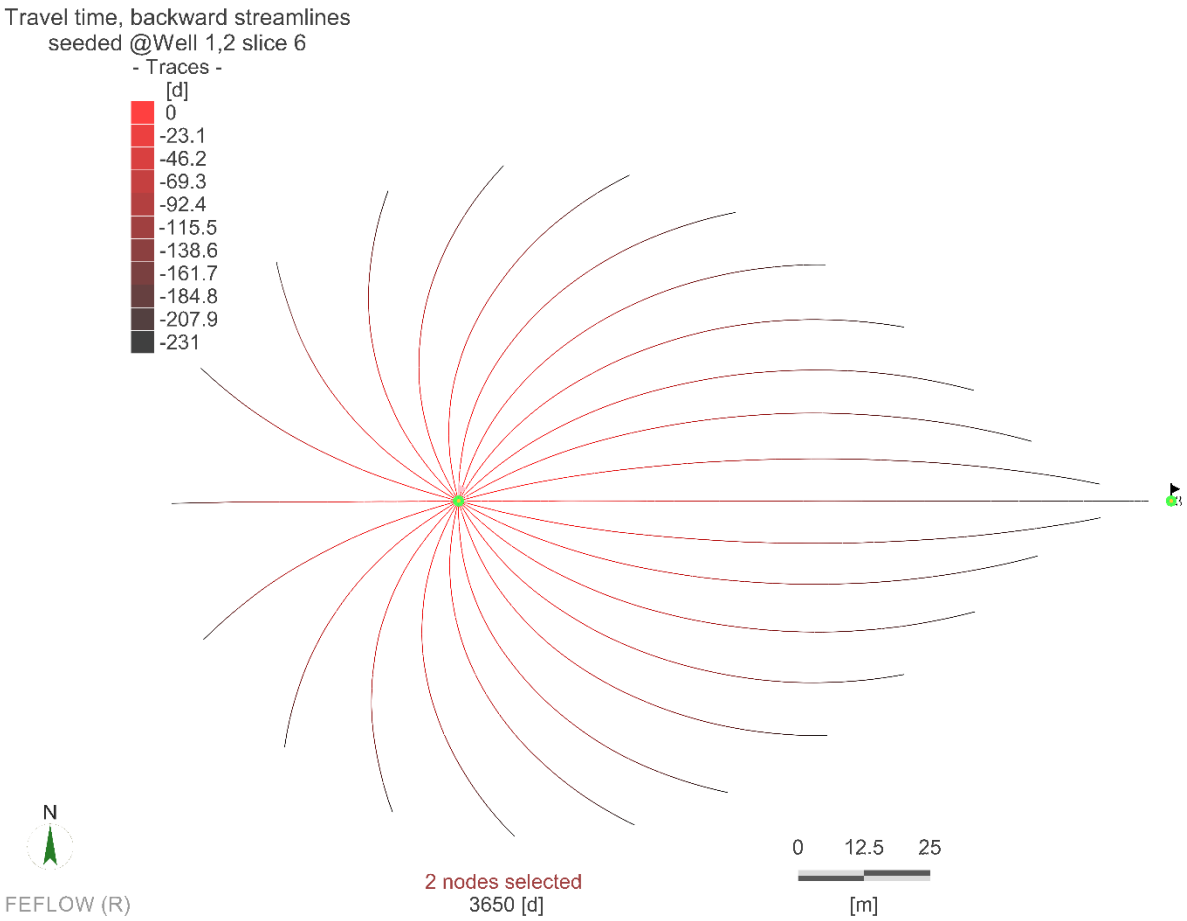
Travel time, backward streamlines
seeded @Well 1,2 slice 6
- Traces -
[d]
0
-23.1
-46.2
-69.3
-92.4
-115.5
-138.6
-161.7
-184.8
-207.9
-231
N
0
12.5
25
[m]
2 nodes selected
3650 [d]
FEFLOW (R)

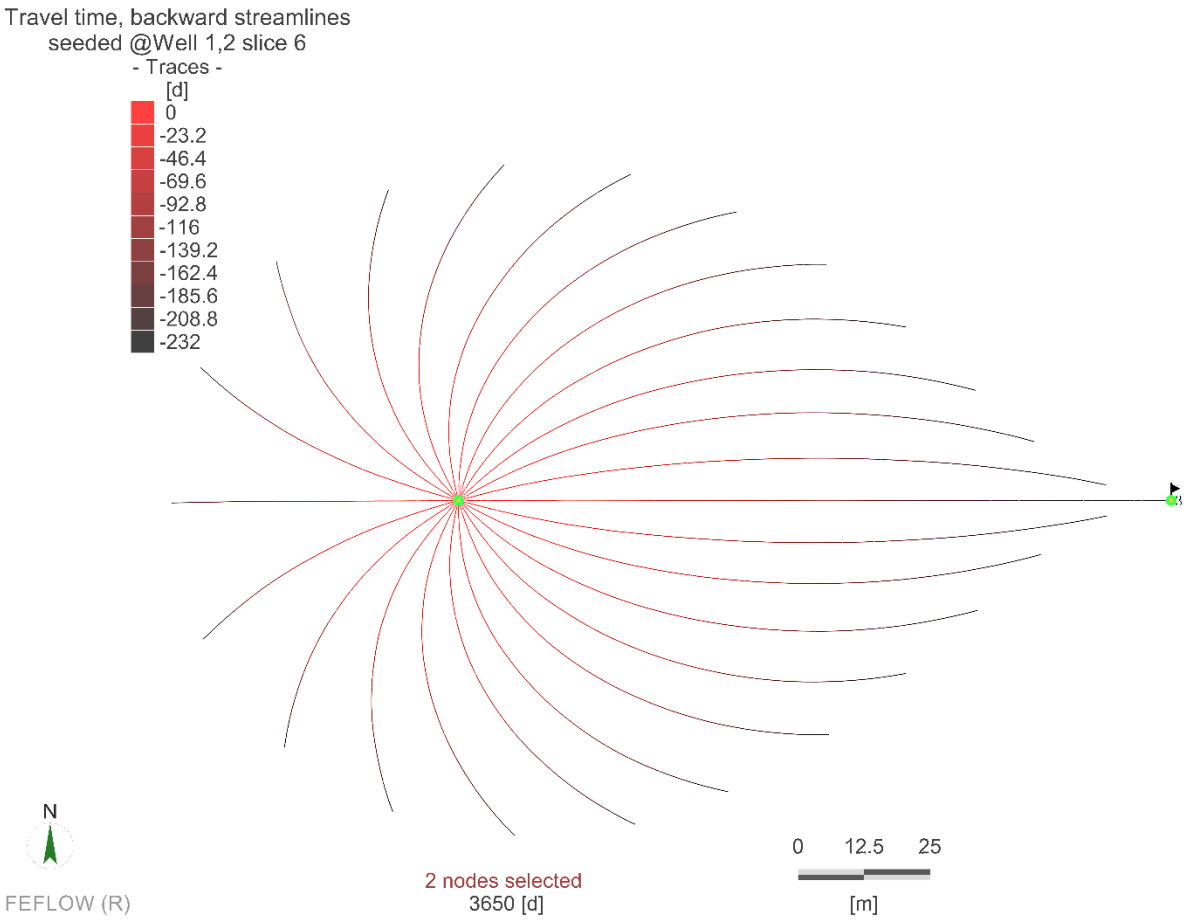
Travel time, backward streamlines
seeded @Well 1,2 slice 6
- Traces -
[d]
0
-23.2
-46.4
-69.6
-92.8
-116
-139.2
-162.4
-185.6
-208.8
-232
N
0
12.5
25
[m]
2 nodes selected
3650 [d]
FEFLOW (R)

Figure 21: Solving hydraulic breakthrough time through streamline method

Take the same hydraulic gradient scenario as an example. streamline method tells that the fluid injected has not reached the abstraction well on day 231 yet reached on day 232 as is shown in Figure 21 which intuitively indicates that t_{hyd}=232 days. Same manner applies for scenarios where abstraction well situate up and down the hydraulic gradient. Corresponding hydraulic breakthrough time is 241 and 224 days respectively (natural flow speed i=5e-8m/s).

Despite the fact that implementing the streamline method is more direct a way and provides a more accurate value in simulation (error is confined to one day and therefore can be viewed as accurate value), such method has to acquire a complete data file in advance which means it must occupy considerable memory and storage space on hard drive (approximately 10G for a 10 year-simulation). In comparison, although employing Darcy's law method will inevitably introduce error to a certain extent, the error can be restrained by increasing the amount of decomposition, i.e. having Δh between two adjacent potentiometric lines smaller. Figure 22 and 23 presents an identical potentiometric surface of the same hydraulic gradient scenario where the only difference is Δh between potentiometric lines is 0.01m in figure 22 and 0.005m in figure 23.

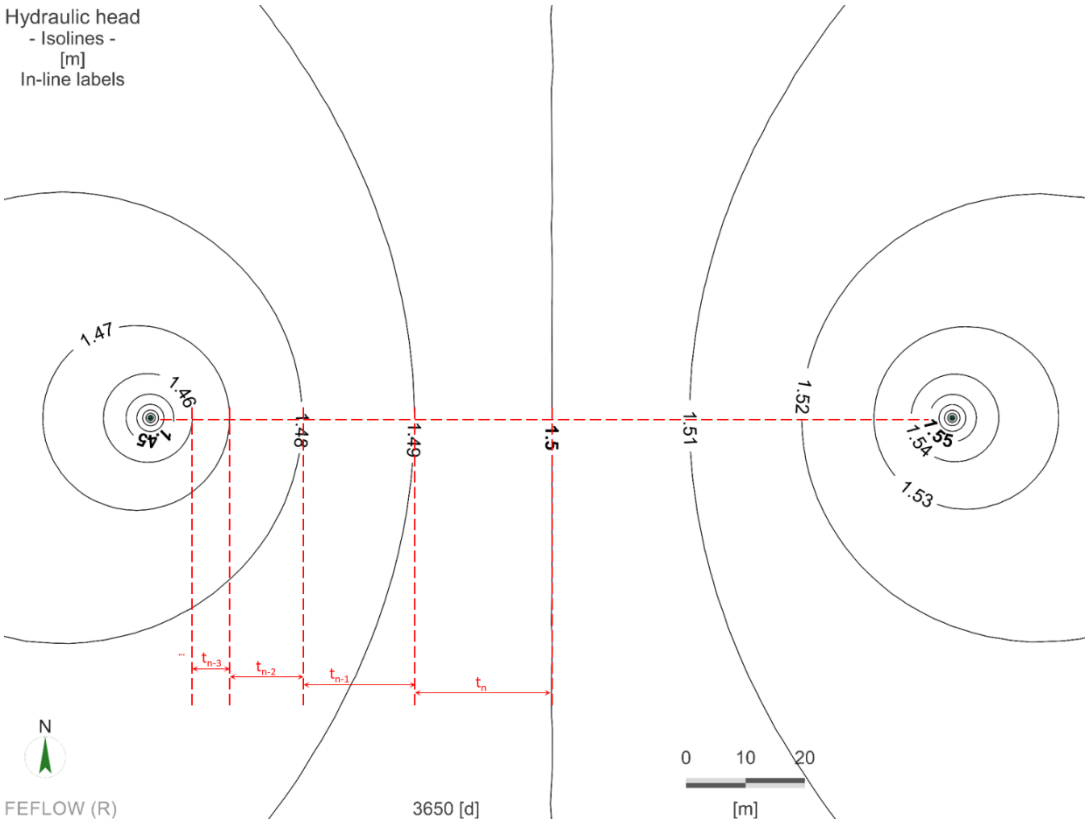

Figure 22: Potentiometric surface (Δh=0.01) to be used in calculating hydraulic breakthrough time by Darcy's law (the same hydraulic gradient scenario)

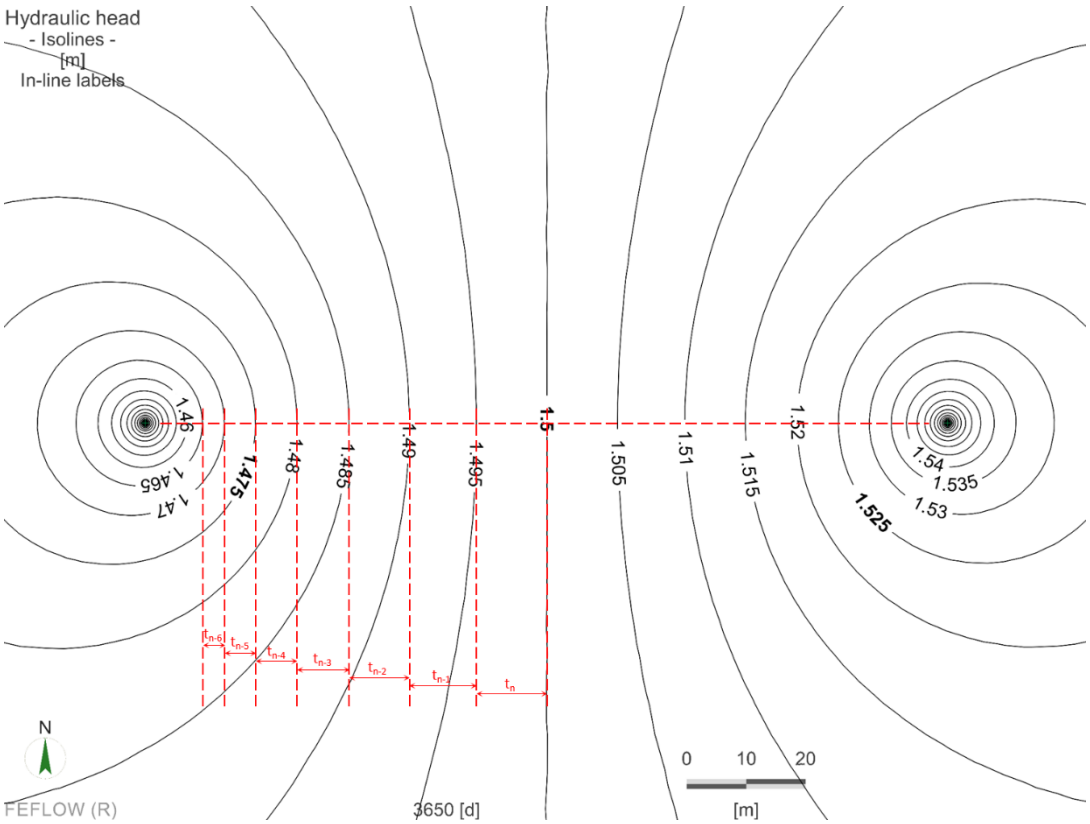

Figure 23: Potentiometric surface (Δh=0.005) to be used in calculating hydraulic breakthrough

time by Darcy's law (the same hydraulic gradient scenario)

Hydraulic breakthrough time calculated by factoring both figures into Darcy's law is 174.4 and 187.7 days. The error evolved comparing to the result from streamline method equals to 24.8% and 19.1% respectively. The outcome implies the fact that a more accurate result can be achieved as long as density of the potentiometric lines is artificially raised on the figure. On the whole, Darcy's law is more convenient a way to calculate hydraulic breakthrough time under limited computational resources.

9.2 Thermal breakthrough time

Temperature at abstraction point, as is presented in figure 24, remains its initial value for a little less than a year until it reaches its thermal breakthrough time and begins to fall drastically until it gradually slows down its downside trend and approaches the Injection temperature over a long period of simulation time.

Owing to the fact that heat is absorbed into mineral grains in flow passage, the heat signal is usually effectively retarded thus having thermal breakthrough time t_{the} significantly left behind hydraulic breakthrough time t_{hyd}.

Likewise, there exists two means for calculating thermal breakthrough time. The first method is conducting a thermal simulation and therefore document the change in abstraction well temperature as is shown in figure 24. Thermal breakthrough time for different relative direction of groundwater flow is found when the abstraction water temperature drops 0.1K from its initial value.

The other method generates an expected thermal breakthrough time t_{the} by multiplying hydraulic breakthrough time by retardation factor R_{the}, i.e.

$$t_{the} = t_{hyd} \cdot R_{the}$$

Where retardation factor $R_{the} = \frac{S_{VCwat}}{S_{VCaq} \cdot n_e} = \frac{2.2}{4.18 \cdot 0.3} = 1.754$ as has been discussed in chapter 4.5. Thermal breakthrough time found from both method and corresponding error is listed in Table 7.

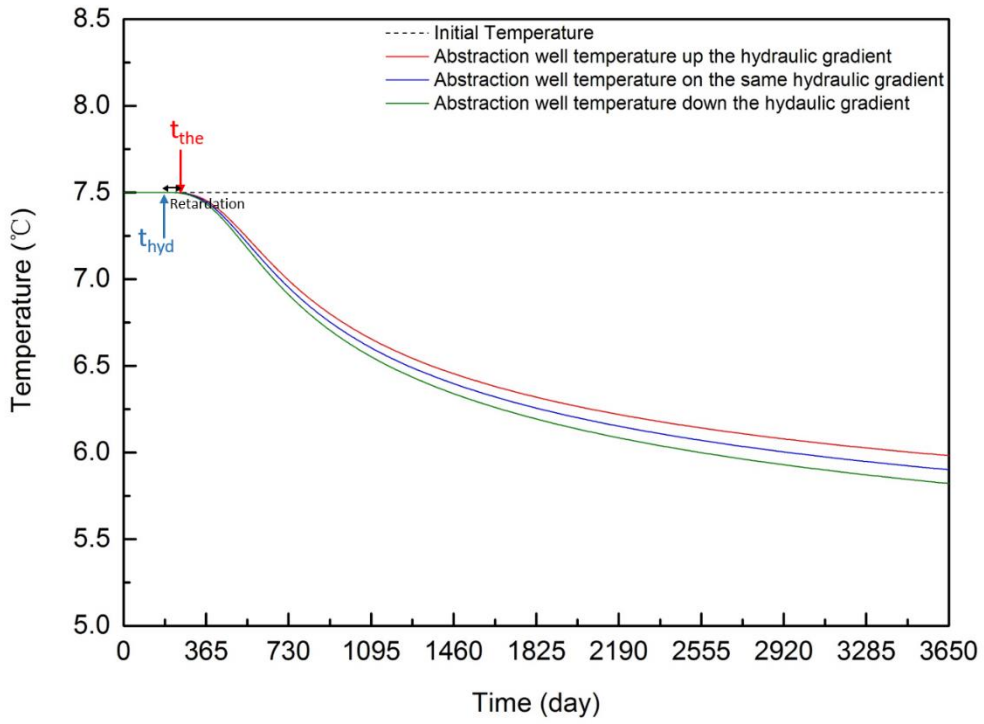

Figure 24: Abstraction well temperature for different relative direction of groundwater flow (Flow speed: 5e-8 m/s)

Table 8: Comparison between predicted and simulated thermal breakthrough time

Abstraction well's relative position to infiltration well	Hydraulic breakthrough time t_{hyd}	Predicted thermal breakthrough time $t_{the} = R_{the} \cdot t_{hyd}$	Thermal breakthrough time t_{the} by simulation	Error ε
Up the hydraulic gradient	241	423	424	0.31%
On the same hydraulic gradient	232	407	410	0.76%
Down the hydraulic gradient	224	393	398	1.28%

The error term in Table 8 implies that the method of multiplying a retardation factor to hydraulic breakthrough time has a satisfying accuracy and can be an optimal alternative for figuring out thermal breakthrough time without conducting a thermal simulation.

9.3 Influence on breakthrough time

9.3.1 Influence of relative direction of groundwater flow

As is revealed in table 8, placing the abstraction well up the hydraulic gradient would produce a 3.4% increment in thermal breakthrough time as compared to same hydraulic gradient's case. On the contrary, placing the abstraction well down the hydraulic gradient would produce 2.9% depletion in thermal breakthrough time. Additionally, data listed simultaneous suggests the relative direction of the slow groundwater flow (5e-8m/s) contributes limited difference in both hydraulic and thermal breakthrough time.

9.3.2 Influence of speed of groundwater flow

Doubling the speed of groundwater flow would yield a 3.3% increment in thermal breakthrough time from 424 days to 438 days if the abstraction well is placed up the hydraulic gradient from the infiltration well. From this point of view, the speed of groundwater flow as well as its relative direction plays an insignificant role in affecting the breakthrough time.

9.3.3 Influence of abstraction rate

Reducing the abstraction rate by half would generate a 107.5% increment in thermal breakthrough time from 424 days to 880 days if the abstraction well is placed up the hydraulic gradient from the infiltration well.

9.3.4 Influence of hydraulic conductivity

Reducing the hydraulic conductivity by half would generate a 80.2% increment in thermal breakthrough time from 410 days to 739 days if the abstraction well is placed on the same hydraulic gradient from the infiltration well. Apparently, abstraction rate along with hydraulic conductivity proves a conspicuous negative correlation with breakthrough time.

9.4 Influence on long-term efficiency

Take the same hydraulic gradient scenario as an example. A comparison between the temperature at abstraction point and a point 5m above it demonstrates little difference in

temperature and corresponding thermal efficiency. However, a comparison between the abstraction point and a point 5m below it tells that the point below has a larger retardation in receiving the heat signal from injection well. Temperature below the abstraction point remains higher than the abstraction point for roughly 1155days (roughly 3 years) yet it turns lower afterwards. Since enthalpy is in proportion to temperature, the phenomenon suggests that system efficiency would be higher before 3 years and lower afterwards if we place the abstraction point deeper than injection level and vice versa.

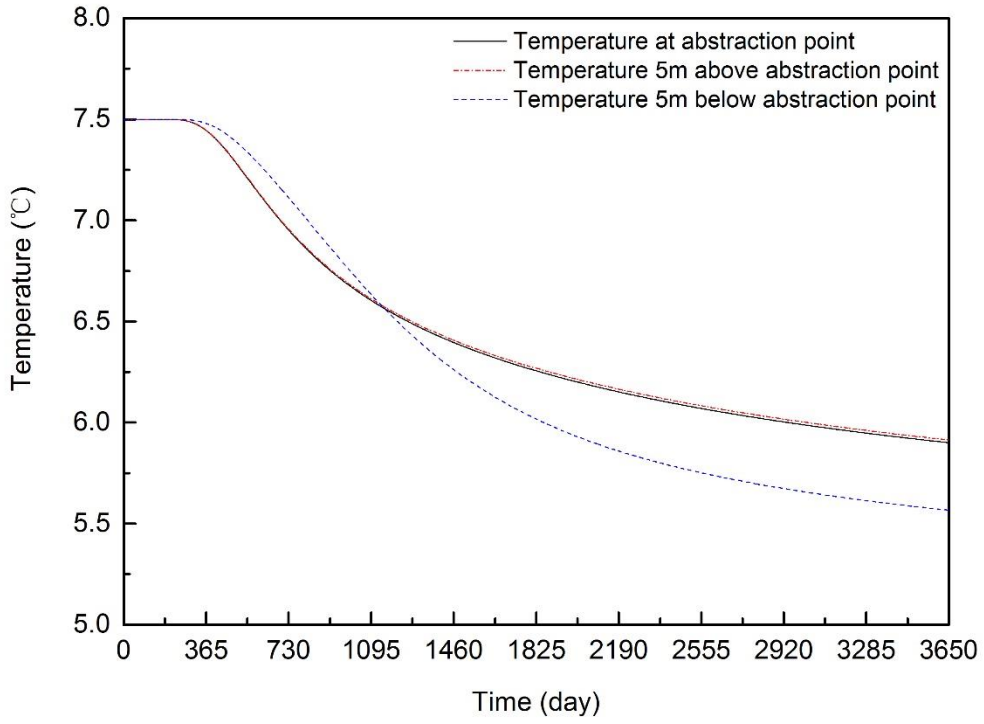

Figure 25: Comparison of temperature change at abstraction point and point 5m above and below

Accordingly, users are recommended to set abstraction point deeper than injection level if short-term efficiency is taken for first priority and place it higher than or at least at the same depth of injection level if long-term efficiency is considered more important.

A simple accumulating carried out on the total enthalpy abstracted implies it turns out to be overall more efficient after 5 years of operation. Since the GWHP system's service life shall be no less than 5 years, users usually don't have to choose between the alternatives.

Once again, factors like speed of groundwater flow, abstraction rate and hydraulic conductivity also have influence on the turning point of transient and overall efficiency. As is displayed in Figure 26 and 27, it's found that speed of groundwater flow as well as relative direction of groundwater flow plays a limited role in altering both turning point. On the contrary, an adjustment made upon either abstraction rate or hydraulic conductivity would incur a significant shift on both turning points. Under such circumstances, the overall efficiency turning point for the system extends to 10 years or more, leaving users the trade-off between short-term and long-term efficiency.

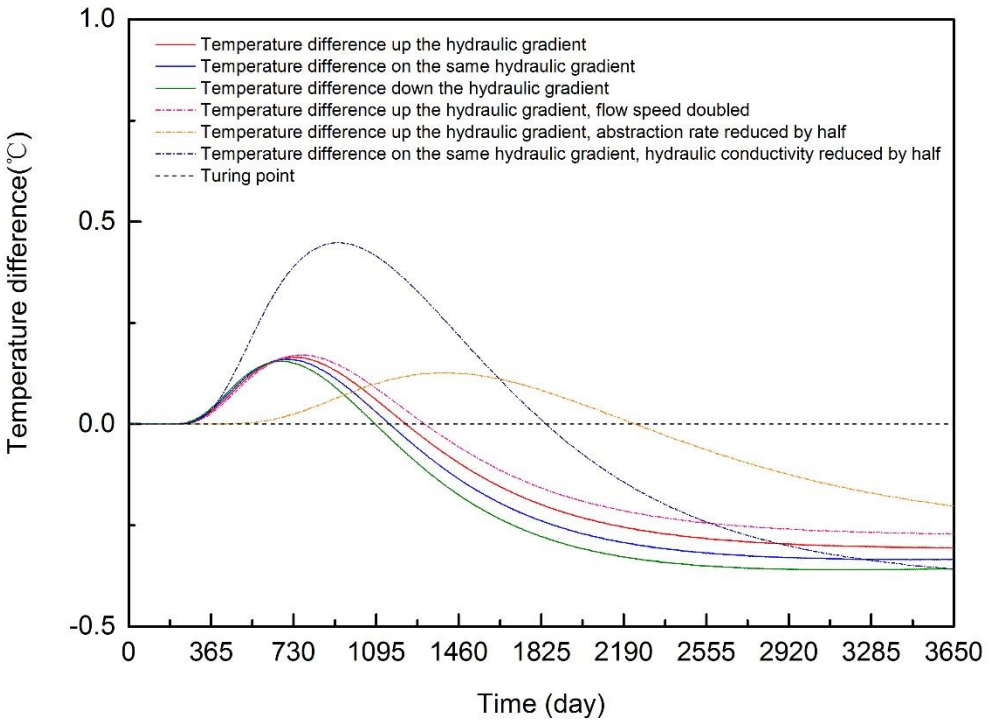

Figure 26: Transient efficiency turning point for different boundary conditions

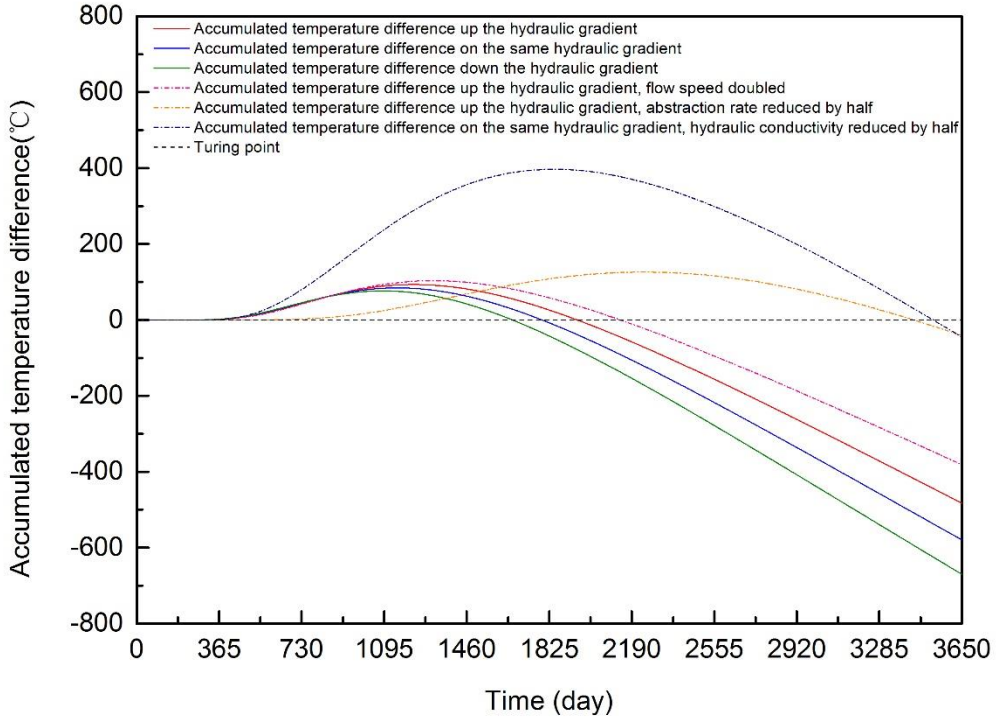

Figure 27: Overall efficiency turning point for different boundary conditions

9.5 Discussion

Placing the abstraction well up the hydraulic gradient produce a case of contrary flow, which more or less helps to delay the breakthrough time. However, the gentle terrain at the fire station restricts the natural flow speed. Whatever direction we choose to arrange production and injection well, we're not expecting to hope that the natural flow making a huge difference in breakthrough time, let alone creating a hydraulic gradient large enough to hold back the entire feedback.

Doubling the speed of the groundwater flow yields the same problem. The original natural flow speed is too inconspicuous. Even if doubling the flow speed creates another "14 days" delay, it corresponds to only another "3.3%" on the large scale.

Yet if wells situate on a precipitous terrain where the natural flow speed i=5e-7m/s rather than 5e-8m/s, the relative direction would have major implications. In a contrary flow situation, the thermal breakthrough would occur after 604 days. However, in a tail flow situation, the breakthrough happens on the 398th day. It would be 206 days or "34.1%" in advance. Under

such circumstances, the direction we choose to arrange the wells would imperatively affect the overall efficiency of the system.

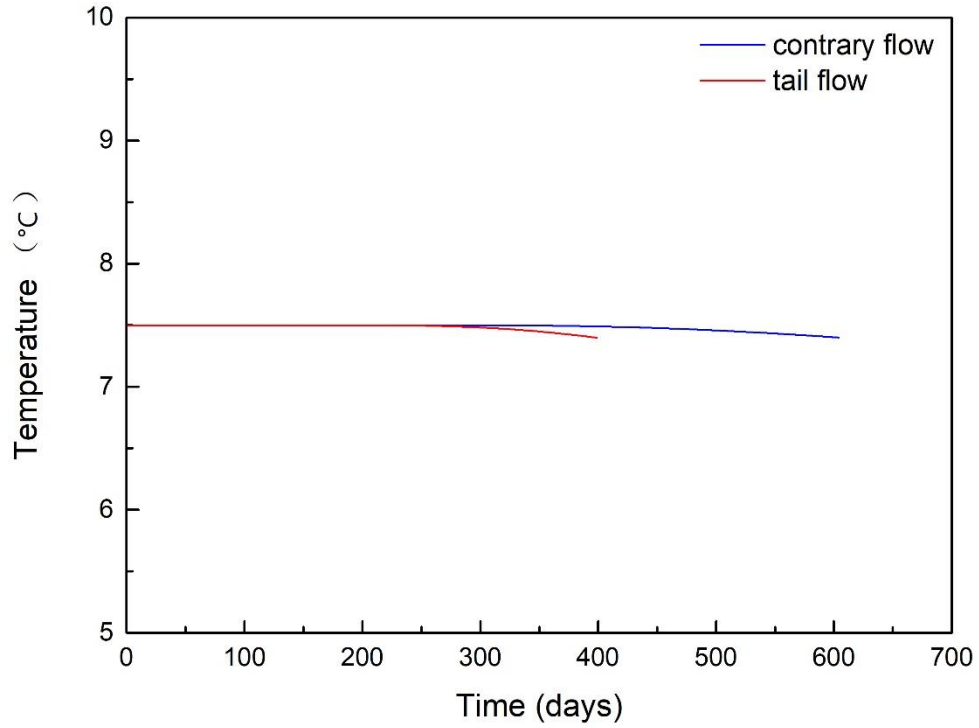

Figure 28: Abstraction well temperature for different relative direction of groundwater flow (Flow speed: 5e-7 m/s)

When it comes to the influence brought by reducing the hydraulic conductivity, it proves to be significant, yet designers are not able to take advantage of it. In fact, wells are deliberately drilled to a level where hydraulic conductivity yields the best.

Similarly, reducing the abstraction rate also seems to contradicts the original intention generates sufficient heat for dwellers. Yet there lies a humble way out of it: put the system into operation in an intermittent manner.

Table 9 displays the weather statistics for Trondheim. Although Trondheim sits in upper latitude, the weather, especially in summer, is not always severely cold. Presuming the GWHP system would only be put into operation when the average temperature of the month submerges beneath 10 degrees Celsius, there would be a 4-month interval before the system runs again.

Table 9: Temperature in Trondheim (www.yr.no Sør-Trøndelag)

Months	Temperature			
	Average	Normal	Warmest	Coldest
Oct-17	6.8°C	5.5°C	15.1°C Oct 3	-0.5°C Oct 20
Sep-17	12.3°C	9.0°C	20.2°C Sep 3	5.2°C Sep 3
Aug-17	13.1°C	12.5°C	21.8°C Aug 6	4.7°C Aug 27
Jul-17	14.0°C	13.0°C	25.6°C Jul 21	4.1°C Jul 6
Jun-17	12.5°C	12.0°C	25.0°C Jun 30	2.3°C Jun 2
May-17	8.5°C	9.0°C	19.2°C May 20	-2.4°C May 10
Apr-17	3.3°C	3.0°C	9.6°C Apr 3	-4.0°C Apr 24
Mar-17	1.0°C	0.0°C	8.5°C Mar 26	-8.4°C Mar 8
Feb-17	-0.7°C	-2.5°C	6.6°C Feb 19	-10.3°C Feb 9
Jan-17	0.9°C	-3.0°C	9.3°C Jan 26	-13.5°C Jan 5
Dec-16	2.1°C	-2.0°C	10.2°C Dec 19	-10.2°C Dec 12
Nov-16	0.3°C	0.5°C	8.9°C Nov 25	-10.9°C Nov 7
Oct-16	4.8°C	5.5°C	14.7°C Oct 7	-3.9°C Oct 12

Taking the interval between two operation cycle into consideration, the input function for boundary condition at multilayer wells are displayed in the figure 29. The system would have a 125-day halt after every 240 days of operation.

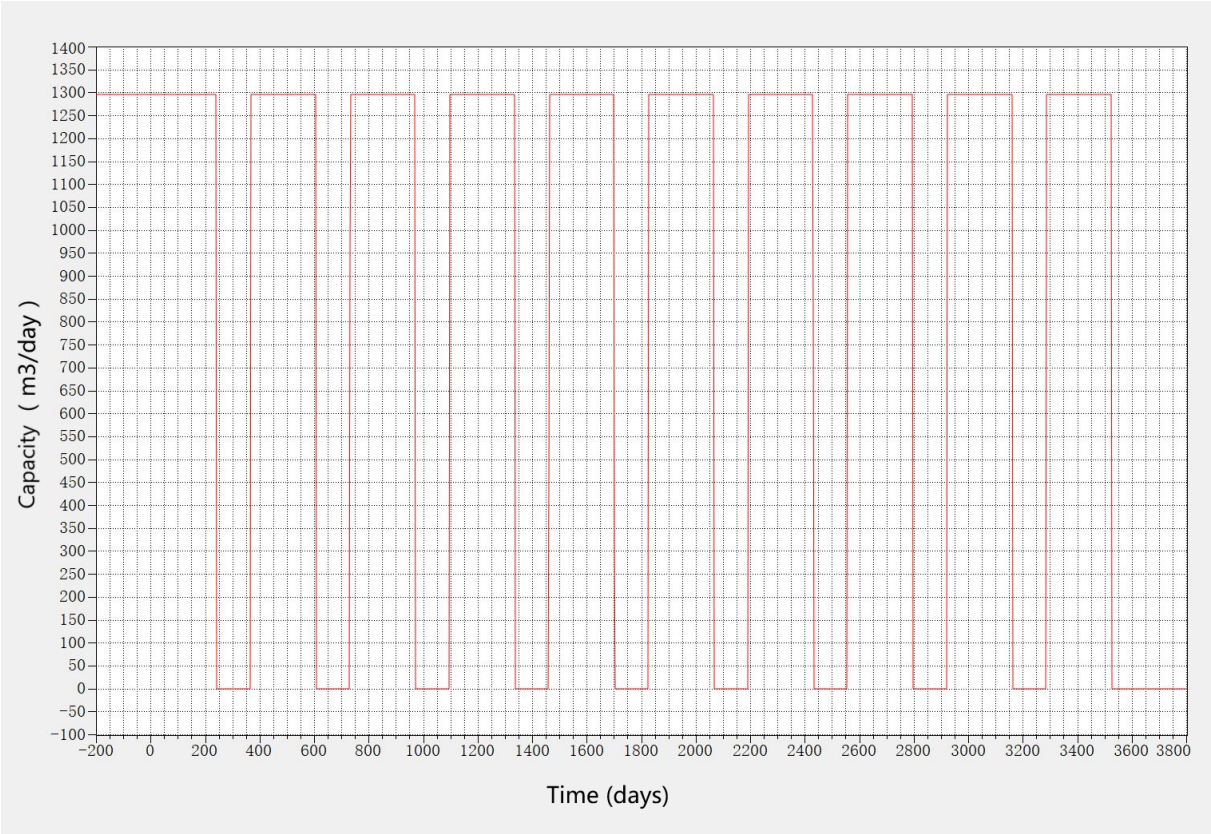

Figure 29: Abstraction well capacity for intermittent operation

Figure 30 reveals the comparison between the system operates in a continuous and intermittent manner. A continuous operation yields a slippery degressive temperature curve while an intermittent operation would produce a temperature upward whenever the system is put into a halt. The upward is more remarkable in later years when temperature at abstraction well is significantly lower comparing to surrounding strata.

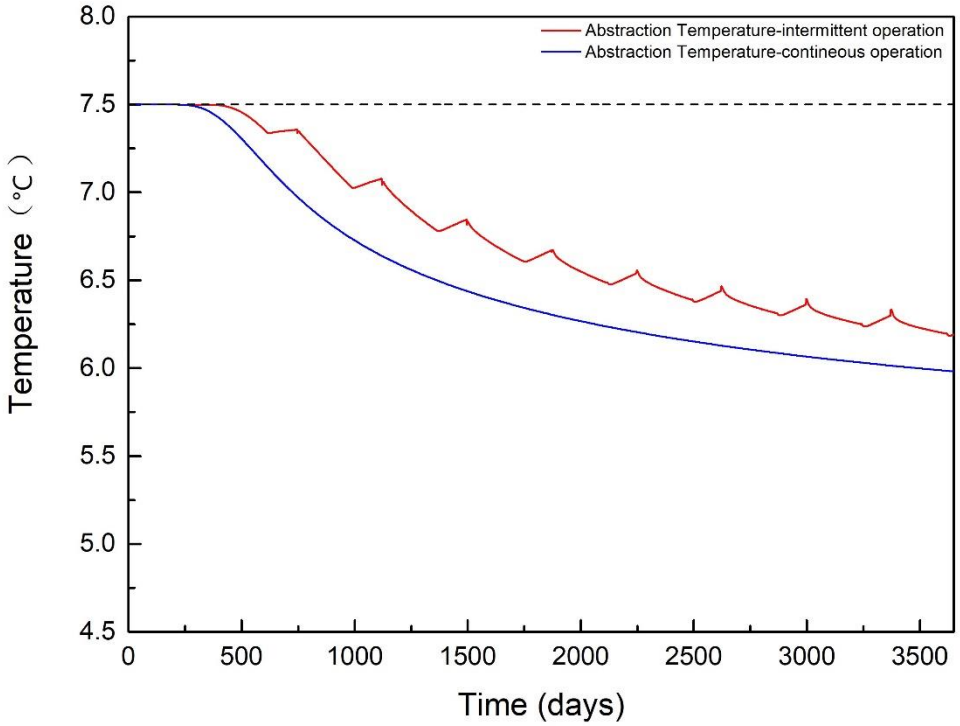

Figure 30: Abstraction well temperature for different relative direction of groundwater flow (Flow speed: 5e-7 m/s)

Intermittent operation brings obvious advantage in thermal efficiency in terms of ending temperature of each operation cycle as is shown in figure 31. The entire temperature difference shapes like a logarithmic normal distribution curve which yields the greatest in the third year after operation and converges afterwards. At the end of the tenth year, the temperature difference between the system operates in a continuous and intermittent manner stands at 0.211 degree Celsius. After 10 years' operation the accumulated difference in heat abstracted would be approximately 3256 GJ.

Table 10: Temperature difference at beginning and end of each operation cycle

Year	1	2	3	4	5	6	7	8	9	10
Temperature Difference-beg	0	0.192	0.299	0.295	0.278	0.262	0.249	0.24	0.232	0.226
Temperature Difference-end	0.045	0.361	0.412	0.373	0.325	0.287	0.26	0.239	0.223	0.211

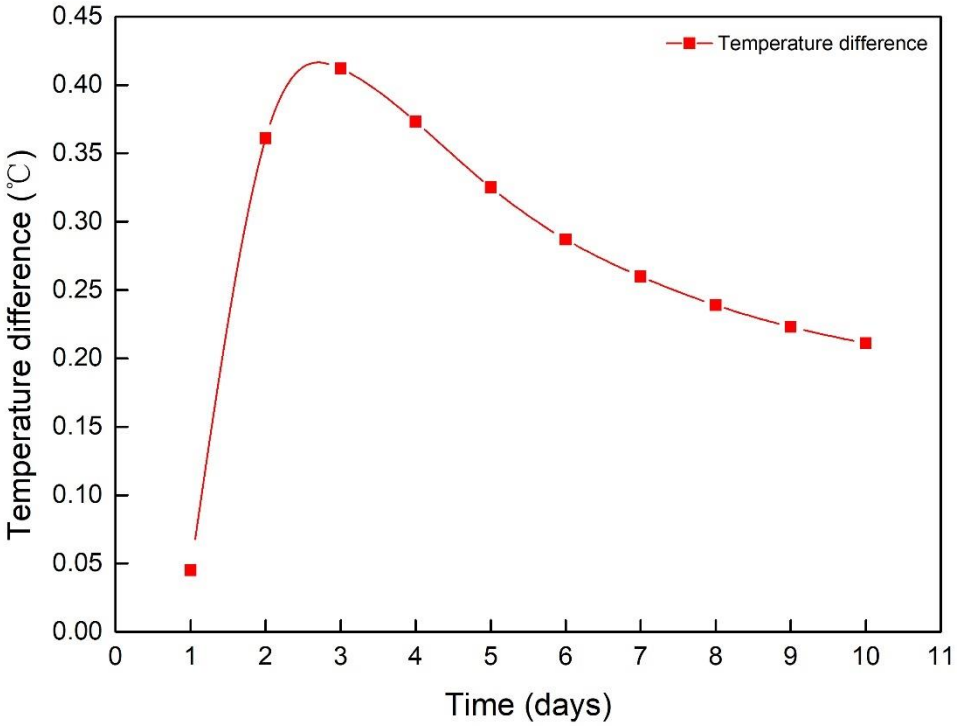

Figure 31: Temperature difference at the end of each operation cycle

From the perspective of thermal breakthrough time, the intermittent manner would postpone the breakthrough till the 562th day from the original 424th day. Excluding the 125-days halt, the heat absorbed from adjacent strata during the halt would account for another 13-days delay in thermal breakthrough.

The accumulated temperature difference between the abstraction point and a point 5m below it is shown in figure 32. It shows that the intermittent operation manner substantially delay the turning point of overall efficiency. Both in a contrary flow situation, the turning point for overall efficiency under continuous operation stands at 1794th day while the turning point for overall efficiency under intermittent operation stands at 2817th day, roughly 8 years after operation.

The large retardation of turning point leaves the users a more likely situation to have to choose between short-term and long-term efficiency. As it has been discussed above, users are recommended to set abstraction point deeper than injection level if short-term efficiency is

taken for first priority and place it higher than or at least at the same depth of injection level if long-term efficiency is considered more important.

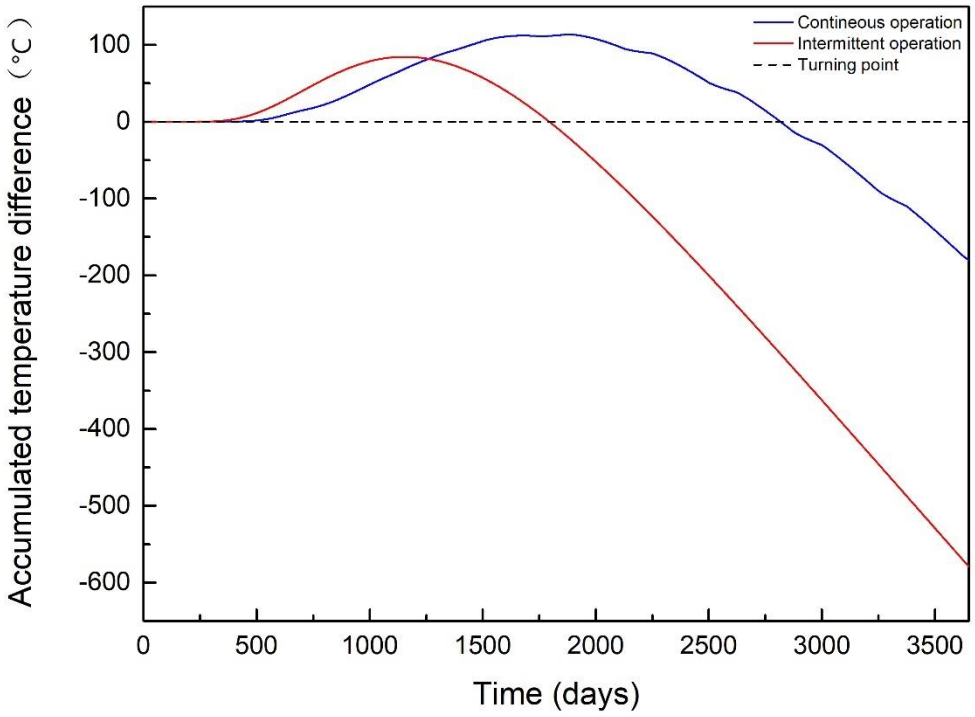

Figure 32: Overall efficiency turning point for continuous and intermittent operation (Contrary flow)

10. Conclusion

The work investigates regional fluid and heat interference between well doublets, thus aiming at provide decision-making reference in selecting critical parameters to delay the adverse impact brought by the thermal interaction. CFD models were established on account of geometric parameters collected form fire station of Melhus with software Feflow, validation was conducted and multiple 10-year simulations were performed accordingly.

Results obtained reveals that:

1. Factoring a steady state potentiometric surface diagram into Darcy's law provides a sturdy alternative for calculating hydraulic breakthrough time with streamline methods under limited computational resources. The method could be further enhanced in accuracy by artificially raising the density of the potentiometric lines on the diagram.
2. Multiplying a retardation factor to an already solved hydraulic breakthrough time can be an optimal alternative of satisfying accuracy for working out the thermal breakthrough time comparing to traditional means of conducting a thermal simulation and documents the inflection point of abstraction temperature.
3. Among the multiple external factors that accounts for altering the breakthrough time and thermal turning points, the speed and relative direction of groundwater flow does not play a decisive role at Melhus fire station where the terrain is generally flat. It indicates that users could choose either well for abstraction or injection without encountering much difference in overall efficiency.
4. A comparison between the temperature trend on abstraction point and a point below it implies the users to situate the abstraction point deeper than injection level if short-term efficiency is considered more important and to place the abstraction point higher than or at least at the same depth of injection level if long-term efficiency values more.
5. Put the GWHP system into operation in an intermittent manner significantly raises the ending temperature at the end of each operation cycle by 0.2-0.4 degrees Celsius. Meanwhile, it also substantially postpones the breakthrough time and thermal turning points for overall efficiency.
6. Under normal circumstances when the GWHP system is put into continuous operation, users

are recommended to place the abstraction point higher than or at least at the same depth of injection level. However, under circumstances where abstraction rate is much lower than 7.5L/s or an intermittent manner of operation is introduced, users usually have to make a trade-off between short-term and long-term efficiency.

List of references

[1] National Bureau of Statics of China. China statistical yearbook-2015[R]. Beijing: China Statistics Press, 2015.

[2] Beier R A, Smith M D, Spitler J D. Reference data sets for vertical borehole ground heat exchanger models and thermal response test analysis[J]. Geothermics, 2011, 40(1): 79-85.

[3] Ball D A, Fischer R D, Hodgett D. Design methods for ground-source heat pumps[R]. Battelle Columbus Labs., OH (USA); Battelle-Institut eV, Frankfurt am Main (Germany, FR), 1983.

[4] Ingersioll L, Zobel O J, Ingersoll A C. Heat Conduction: With Engineering Geological And Other Applications[J]. 1954.

[5] Kavanaugh S P. A design method for hybrid ground-source heat pumps[J]. ASHRAE transactions, 1998, 104: 691.

[6] Kavanaugh S, Gilbreath C, Kilpatrick J. Cost Containment for Ground-source Heat Pumps. Final Reports[R]. University of Alabama, 1995.

[7] OWNER G H P. An information survival kit for the prospective geothermal heat pump owner[J]. 2001.

[8] Yang H, Cui P, Fang Z. Vertical-borehole ground-coupled heat pumps: A review of models and systems[J]. Applied Energy, 2010, 87(1): 16-27.

[9] Carslaw H S, Jaeger J C. Conduction of heat in solids[J]. Oxford: Clarendon Press, 1959, 2nd ed., 1959.

[10] Shonder J A, Baxter V, Thornton J, et al. A new comparison of vertical ground heat exchanger design methods for residential applications[J]. ASHRAE Transactions, 1999, 105: 1179.

[11] Banks D. An introduction to thermogeology: ground source heating and cooling[M]. John Wiley & Sons, 2012.

[12] Papadopulos I S, Cooper H H. Drawdown in a well of large diameter[J]. Water Resources Research, 1967, 3(1): 241-244.

[13] Tartakovsky G D, Neuman S P. Three‐dimensional saturated‐unsaturated flow with

axial symmetry to a partially penetrating well in a compressible unconfined aquifer[J]. Water Resources Research, 2007, 43(1).

[14] Clyde C G, Madabhushi G V. Spacing of wells for heat pumps[J]. Journal of Water Resources Planning and Management, 1983, 109(3): 203-212.

[15] Fetter C W. Applied hydrogeology[M]. Prentice hall, 2000.

[16] Grove D B, Beetem W A. Porosity and dispersion constant calculations for a fractured carbonate aquifer using the two well tracer method[J]. Water Resources Research, 1971, 7(1): 128-134.

[17] Luo J, Kitanidis P K. Fluid residence times within a recirculation zone created by an extraction–injection well pair[J]. Journal of Hydrology, 2004, 295(1): 149-162.

[18] De Marsily G. Quantitative hydrogeology[R]. Paris School of Mines, Fontainebleau, 1986.

[19] Ingersoll L R, Plass H J. Theory of the ground pipe heat source for the heat pump[J]. ASHVE transactions, 1948, 47(7): 339-348.

[20] Marcotte D, Pasquier P, Sheriff F, et al. The importance of axial effects for borehole design of geothermal heat-pump systems[J]. Renewable Energy, 2010, 35(4): 763-770.

[21] Zeng H Y, Diao N R, Fang Z H. A finite line‐source model for boreholes in geothermal heat exchangers[J]. Heat Transfer—Asian Research, 2002, 31(7): 558-567.

[22] Molina-Giraldo N, Blum P, Zhu K, et al. A moving finite line source model to simulate borehole heat exchangers with groundwater advection[J]. International Journal of Thermal Sciences, 2011, 50(12): 2506-2513.

[23] Jaeger J C. Conduction of heat in an infinite region bounded internally by a circular cylinder of a perfect conductor[J]. Australian Journal of Physics, 1956, 9(2): 167-179.

[24] Eskilson P. Thermal analysis of heat extraction boreholes[M]. 1987.

[25] He M, Rees S, Shao L. Simulation of a domestic ground source heat pump system using a three-dimensional numerical borehole heat exchanger model[J]. Journal of Building Performance Simulation, 2011, 4(2): 141-155.

[26] Hecht Méndez, Jozsef, et al. Evaluating MT3DMS for heat transport simulation of closed geothermal systems[M]. Ground water, 2010, 48(5): 741-756.

[27] Li Z. A new constant heat flux model for vertical U-tube ground heat exchangers[J]. Energy and Buildings, 2012, 45: 311-316.

[28] Stefano Lo Russoa, Glenda Taddiaa, Vittorio Verdab. Development of the thermally affected zone (TAZ) around a groundwater heat pump (GWHP) system: A sensitivity analysis[J] Geothermics, 2012, 43: 66-74.

[29] Wei Y, Ende W. Example for the Simulation of Groundwater Flow Based on AQUA3D [J]. Geotechnical Investigation & Surveying, 2004, 3: 008.

[30] Deng Z. Modeling of standing column wells in ground source heat pump systems[D]. Oklahoma State University, 2004.

[31] Fujii H, Itoi R, Fujii J, et al. Optimizing the design of large-scale ground-coupled heat pump systems using groundwater and heat transport modeling[J]. Geothermics, 2005, 34(3): 347-364.

[32] Russo S L, Civita M V. Open-loop groundwater heat pumps development for large buildings: a case study[J]. Geothermics, 2009, 38(3): 335-345.

[33] BRATTLI, B. 2009a. Fysisk og kjemisk hydrogeologi, Norges teknisk-naturvitenskapelige universitet.

[34] Williams P J. Determination of heat capacities of freezing soils[C]//Symposium on Frost Action on Roads, Paris (1973). 1973, 1

Appendix

Udf functions for validation

```
#include"udf.h"

DEFINE_PROFILE(InletVelocity, thread, position)
{
	face_t f;
	real velo;
	real t = RP_Get_Real("flow-time");
	real tstep = RP_Get_Real("physical-time-step");

	int i=0;

	real velocity[2832]={0.000, 0.346...};
	begin_f_loop(f, thread)
	{
		i = floor(t/tstep);
		velo = velocity[i];
		F_PROFILE(f, thread, position) = velo;
	}
	end_f_loop(f, thread)
}

DEFINE_PROFILE(InletTemperature, thread, position)
{
	face_t f;
	real Temp;
	real t = RP_Get_Real("flow-time");
	real tstep = RP_Get_Real("physical-time-step");

	int i=0;

	real temperature[2832]={295.361, 296.050...};
	begin_f_loop(f, thread)
	{
		i = floor(t/tstep);
		Temp = temperature[i];
		F_PROFILE(f, thread, position) = Temp;
	}
	end_f_loop(f, thread)
}
```

C++function for extracting data from output files

```
#include <iostream>
#include <cstring>
#include <cstdio>
#include <cstdlib>
using namespace std;

char empty[100];
double data[3650];

int main() {
	freopen("in.txt", "r", stdin);
	freopen("output.txt", "w", stdout);

	for (int i = 0; i < 3650; i++) {
		cin>>empty;
		cin>>empty;
		cin>>data[i];
		cin>>empty;
	 }

	for (int i = 0; i < 3650; i++){
		printf("%.3f\n", data[i]);
	}

	fclose(stdin);
	fclose(stdout);
	return 0;
}
```

Functions for extracting data

Function 1:

```
#include <iostream>
#include <cstring>
#include <cstdio>
#include <cstdlib>
using namespace std;

char empty[100];
double data[200];

int main() {
	freopen("in.txt", "r", stdin);
	freopen("output.txt", "w", stdout);

	for (int i = 0; i < 200; i++) {
		cin>>empty;
		  cin>>empty;
		  cin>>data[i];
		  cin>>empty;
	 }

	for (int i = 0; i < 200; i++){
		  printf("%.3f\n", data[i]);
	}

	fclose(stdin);
	fclose(stdout);
	return 0;
}
```

Function 2:

```
#include <iostream>
#include <cstring>
#include <cstdio>
#include <cstdlib>
using namespace std;

char empty[100];
double data[3650];
double tmp;
double out[3650]={0};

int main() {
	freopen("in.txt", "r", stdin);
	freopen("output.txt", "w", stdout);

	for (int i = 0; i < 3650; i++) {
		cin>>data[i];
	 }

	 for (int i = 0; i < 3650; i++){
		for (int j = 0; j <= i; j++){
			tmp += data[j];
		}
		out[i] = tmp;
		tmp=0;
	 }

	for (int i = 0; i < 3650; i++){
		printf("%.3f\n", out[i]);
	}

	fclose(stdin);
	fclose(stdout);
	return 0;
}
```

Horizontal conductivity at Melhus fire station(Gustafsson method is adopted in modelling)

Monitor depth	Hazen method (m/s)	Gustafsson method (m/s)	Harleman method (m/s)	U.S. Berau method (m/s)
12m	1.7E-04	3.31E-05	8.65E-07	6.82E-04
15m	3.99E-04	1.74E-04	2.94E-06	1.13E-03
18m	1.87E-02	2.31E-02	1.38E-04	4.51E-03
21m	3.18E-03	2.18E-03	2.34E-05	1.70E-03
24m	7.33E-04	6.69E-04	5.40E-06	1.02E-04
27m	3.00E-03	2.40E-03	2.21E-05	6.37E-04
30m	2.13E-04	1.49E-04	1.57E-06	2.45E-05
33m	6.63E-04	6.07E-04	4.89E-06	1.18E-04
36m	8.14E-04	9.04E-04	6.00E-06	1.02E-04
38m	5.47E-04	5.74E-04	4.03E-06	6.32E-05
39m	1.23E-03	1.43E-03	9.10E-06	1.25E-04
41m	1.55E-03	1.68E-03	1.15E-05	2.21E-04
42m	1.08E-03	1.16E-03	7.98E-06	1.26E-04
44m	2.22E-04	2.23E-04	1.64E-06	2.15E-05
45m	4.55E-04	4.84E-04	3.35E-06	4.83E-05
47m	6.74E-04	8.18E-04	4.97E-06	6.29E-05
48m	1.25E-03	1.06E-03	9.22E-06	2.16E-04
50m	7.85E-04	6.91E-04	5.79E-06	8.85E-05
51m	1.01E-03	1.15E-03	7.44E-06	1.21E-04
53m	1.19E-03	9.62E-04	8.78E-06	1.82E-04
54m	2.49E-03	2.97E-03	1.84E-05	3.29E-04
56m	3.70E-03	4.63E-03	2.73E-05	4.89E-04
57m	1.11E-02	1.37E-02	8.18E-05	1.83E-03
59m	1.72E-03	1.63E-03	1.27E-05	2.78E-04
60m	1.45E-03	1.63E-03	1.07E-05	1.59E-04
62m	1.31E-03	1.61E-03	9.69E-06	1.44E-04
63m	8.56E-04	1.17E-03	6.32E-06	8.21E-05
65m	6.84E-04	4.86E-04	5.05E-06	1.24E-04
66m	2.71E-03	2.68E-03	2.00E-05	4.58E-04
67m	6.72E-04	6.70E-04	4.96E-06	6.20E-05
68m	3.20E-04	4.00E-04	2.36E-06	2.86E-05

Key performance data for calculating thermal break through time t_{the}:

Words abbreviated are listed as follow:
D: Days
C: Temperature at abstraction point for a Contrary flow.
S: Temperature at abstraction point for a Stationary flow.
T: Temperature at abstraction point for a Tail flow.
A: Auxiliary temperature for a difference to be detected.
CI: Temperature at abstraction point for a Contrary flow where the flow speed for groundwater is doubled.
CK: Temperature at abstraction point for a Contrary flow where the conductivity is reduced by half.
DC: Difference between temperature of Contrary flow and Auxiliary temperature.
DS: Difference between temperature of Stationary flow and Auxiliary temperature.
DT: Difference between temperature of Tail flow and Auxiliary temperature.
DCI: Difference between temperature of a Contrary flow where the flow speed for groundwater is doubled and Auxiliary temperature.
DCK: Difference between temperature of a Contrary flow where the conductivity is reduced by half and Auxiliary temperature.

Crucial data for calculating thermal break through time for different relative direction of groundwater flow (flow speed: 5e-8m/s)

D	C	S	T	A	DC	DS	DT	CI	DCI	CK	DCK
1	7.50	7.50	7.50	7.40	0.10	0.10	0.10	7.50	0.10	7.50	0.10
…	…	…	…	…	…	…	…	…	…	…	…
250	7.50	7.50	7.50	7.40	0.10	0.10	0.10	7.50	0.10	7.50	0.10
390	7.43	7.42	7.41	7.40	0.03	0.02	0.01	7.44	0.04	7.46	0.06
391	7.43	7.42	7.41	7.40	0.03	0.02	0.01	7.44	0.04	7.46	0.06
392	7.43	7.42	7.41	7.40	0.03	0.02	0.01	7.44	0.04	7.46	0.05
393	7.43	7.42	7.41	7.40	0.03	0.02	0.00	7.44	0.04	7.46	0.05
394	7.43	7.42	7.40	7.40	0.03	0.02	0.00	7.44	0.04	7.45	0.05
395	7.43	7.42	7.40	7.40	0.03	0.02	0.00	7.44	0.04	7.45	0.05
396	7.43	7.42	7.40	7.40	0.03	0.02	0.00	7.44	0.04	7.45	0.05
397	7.43	7.41	7.40	7.40	0.03	0.01	0.00	7.44	0.04	7.45	0.05
398	7.43	7.41	7.40	7.40	0.03	0.01	0.00	7.44	0.04	7.45	0.05
399	7.43	7.41	7.40	7.40	0.02	0.01	0.00	7.44	0.04	7.45	0.05
400	7.42	7.41	7.40	7.40	0.02	0.01	0.00	7.44	0.04	7.45	0.05
401	7.42	7.41	7.40	7.40	0.02	0.01	0.00	7.44	0.03	7.45	0.05
402	7.42	7.41	7.40	7.40	0.02	0.01	-0.01	7.43	0.03	7.45	0.05
403	7.42	7.41	7.39	7.40	0.02	0.01	-0.01	7.43	0.03	7.45	0.05
404	7.42	7.41	7.39	7.40	0.02	0.01	-0.01	7.43	0.03	7.45	0.05
405	7.42	7.41	7.39	7.40	0.02	0.01	-0.01	7.43	0.03	7.45	0.05
406	7.42	7.41	7.39	7.40	0.02	0.00	-0.01	7.43	0.03	7.45	0.04
407	7.42	7.40	7.39	7.40	0.02	0.00	-0.01	7.43	0.03	7.44	0.04

408	7.42	7.40	7.39	7.40	0.02	0.00	-0.01	7.43	0.03	7.44	0.04
409	7.42	7.40	7.39	7.40	0.01	0.00	-0.01	7.43	0.03	7.44	0.04
410	7.41	7.40	7.39	7.40	0.01	0.00	-0.02	7.43	0.03	7.44	0.04
411	7.41	7.40	7.38	7.40	0.01	0.00	-0.02	7.43	0.03	7.44	0.04
412	7.41	7.40	7.38	7.40	0.01	0.00	-0.02	7.43	0.02	7.44	0.04
413	7.41	7.40	7.38	7.40	0.01	0.00	-0.02	7.42	0.02	7.44	0.04
414	7.41	7.40	7.38	7.40	0.01	0.00	-0.02	7.42	0.02	7.44	0.04
415	7.41	7.39	7.38	7.40	0.01	-0.01	-0.02	7.42	0.02	7.44	0.04
416	7.41	7.39	7.38	7.40	0.01	-0.01	-0.02	7.42	0.02	7.44	0.04
417	7.41	7.39	7.38	7.40	0.01	-0.01	-0.02	7.42	0.02	7.44	0.04
418	7.41	7.39	7.38	7.40	0.01	-0.01	-0.03	7.42	0.02	7.44	0.03
419	7.41	7.39	7.37	7.40	0.00	-0.01	-0.03	7.42	0.02	7.43	0.03
420	7.40	7.39	7.37	7.40	0.00	-0.01	-0.03	7.42	0.02	7.43	0.03
421	7.40	7.39	7.37	7.40	0.00	-0.01	-0.03	7.42	0.02	7.43	0.03
422	7.40	7.39	7.37	7.40	0.00	-0.01	-0.03	7.42	0.02	7.43	0.03
423	7.40	7.39	7.37	7.40	0.00	-0.02	-0.03	7.42	0.01	7.43	0.03
424	7.40	7.38	7.37	7.40	0.00	-0.02	-0.03	7.41	0.01	7.43	0.03
425	7.40	7.38	7.37	7.40	0.00	-0.02	-0.04	7.41	0.01	7.43	0.03
426	7.40	7.38	7.36	7.40	0.00	-0.02	-0.04	7.41	0.01	7.43	0.03
427	7.40	7.38	7.36	7.40	0.00	-0.02	-0.04	7.41	0.01	7.43	0.03
428	7.40	7.38	7.36	7.40	-0.01	-0.02	-0.04	7.41	0.01	7.43	0.03
429	7.39	7.38	7.36	7.40	-0.01	-0.02	-0.04	7.41	0.01	7.43	0.03
430	7.39	7.38	7.36	7.40	-0.01	-0.02	-0.04	7.41	0.01	7.43	0.02
431	7.39	7.38	7.36	7.40	-0.01	-0.03	-0.04	7.41	0.01	7.42	0.02
432	7.39	7.37	7.36	7.40	-0.01	-0.03	-0.04	7.41	0.01	7.42	0.02
433	7.39	7.37	7.35	7.40	-0.01	-0.03	-0.05	7.41	0.00	7.42	0.02
434	7.39	7.37	7.35	7.40	-0.01	-0.03	-0.05	7.40	0.00	7.42	0.02
435	7.39	7.37	7.35	7.40	-0.01	-0.03	-0.05	7.40	0.00	7.42	0.02
436	7.39	7.37	7.35	7.40	-0.01	-0.03	-0.05	7.40	0.00	7.42	0.02
437	7.39	7.37	7.35	7.40	-0.02	-0.03	-0.05	7.40	0.00	7.42	0.02
438	7.38	7.37	7.35	7.40	-0.02	-0.03	-0.05	7.40	0.00	7.42	0.02
439	7.38	7.37	7.35	7.40	-0.02	-0.04	-0.05	7.40	0.00	7.42	0.02
440	7.38	7.36	7.35	7.40	-0.02	-0.04	-0.06	7.40	0.00	7.42	0.01
441	7.38	7.36	7.34	7.40	-0.02	-0.04	-0.06	7.40	0.00	7.41	0.01
442	7.38	7.36	7.34	7.40	-0.02	-0.04	-0.06	7.40	0.00	7.41	0.01
443	7.38	7.36	7.34	7.40	-0.02	-0.04	-0.06	7.40	-0.01	7.41	0.01
444	7.38	7.36	7.34	7.40	-0.02	-0.04	-0.06	7.39	-0.01	7.41	0.01
445	7.38	7.36	7.34	7.40	-0.02	-0.04	-0.06	7.39	-0.01	7.41	0.01
446	7.37	7.36	7.34	7.40	-0.03	-0.04	-0.06	7.39	-0.01	7.41	0.01
447	7.37	7.36	7.34	7.40	-0.03	-0.04	-0.07	7.39	-0.01	7.41	0.01
448	7.37	7.35	7.33	7.40	-0.03	-0.05	-0.07	7.39	-0.01	7.41	0.01
449	7.37	7.35	7.33	7.40	-0.03	-0.05	-0.07	7.39	-0.01	7.41	0.01
450	7.37	7.35	7.33	7.40	-0.03	-0.05	-0.07	7.39	-0.01	7.41	0.01

451	7.37	7.35	7.33	7.40	-0.03	-0.05	-0.07	7.39	-0.01	7.41	0.00
452	7.37	7.35	7.33	7.40	-0.03	-0.05	-0.07	7.39	-0.02	7.40	0.00
453	7.37	7.35	7.33	7.40	-0.03	-0.05	-0.07	7.38	-0.02	7.40	0.00
454	7.37	7.35	7.32	7.40	-0.04	-0.06	-0.08	7.38	-0.02	7.40	0.00
455	7.36	7.34	7.32	7.40	-0.04	-0.06	-0.08	7.38	-0.02	7.40	0.00
456	7.36	7.34	7.32	7.40	-0.04	-0.06	-0.08	7.38	-0.02	7.40	0.00
457	7.36	7.34	7.32	7.40	-0.04	-0.06	-0.08	7.38	-0.02	7.40	0.00
458	7.36	7.34	7.32	7.40	-0.04	-0.06	-0.08	7.38	-0.02	7.40	0.00
459	7.36	7.34	7.32	7.40	-0.04	-0.06	-0.08	7.38	-0.02	7.40	0.00
460	7.36	7.34	7.32	7.40	-0.04	-0.06	-0.08	7.38	-0.02	7.40	-0.01

Crucial data for calculating thermal break through time for different relative direction of groundwater flow (flow speed: 5e-7m/s)

Time	contrary flow	tail flow	Time	contrary flow	tail flow	Time	contrary flow	tail flow	Time	contrary flow
days	℃	℃	days	℃	℃	days	℃	℃	days	℃
1	7.5	7.5	152	7.5	7.5	303	7.499	7.48	454	7.476
2	7.5	7.5	153	7.5	7.5	304	7.499	7.479	455	7.475
3	7.5	7.5	154	7.5	7.5	305	7.499	7.479	456	7.475
4	7.5	7.5	155	7.5	7.5	306	7.499	7.478	457	7.475
5	7.5	7.5	156	7.5	7.5	307	7.499	7.478	458	7.474
6	7.5	7.5	157	7.5	7.5	308	7.499	7.477	459	7.474
7	7.5	7.5	158	7.5	7.5	309	7.499	7.477	460	7.474
8	7.5	7.5	159	7.5	7.5	310	7.499	7.476	461	7.473
9	7.5	7.5	160	7.5	7.5	311	7.499	7.476	462	7.473
10	7.5	7.5	161	7.5	7.5	312	7.499	7.475	463	7.473
11	7.5	7.5	162	7.5	7.5	313	7.499	7.475	464	7.472
12	7.5	7.5	163	7.5	7.5	314	7.499	7.474	465	7.472
13	7.5	7.5	164	7.5	7.5	315	7.499	7.474	466	7.472
14	7.5	7.5	165	7.5	7.5	316	7.499	7.473	467	7.471
15	7.5	7.5	166	7.5	7.5	317	7.499	7.473	468	7.471
16	7.5	7.5	167	7.5	7.5	318	7.499	7.472	469	7.471
17	7.5	7.5	168	7.5	7.5	319	7.499	7.471	470	7.47
18	7.5	7.5	169	7.5	7.5	320	7.499	7.471	471	7.47
19	7.5	7.5	170	7.5	7.5	321	7.499	7.47	472	7.469
20	7.5	7.5	171	7.5	7.5	322	7.499	7.469	473	7.469
21	7.5	7.5	172	7.5	7.5	323	7.498	7.469	474	7.469
22	7.5	7.5	173	7.5	7.5	324	7.498	7.468	475	7.468
23	7.5	7.5	174	7.5	7.5	325	7.498	7.468	476	7.468
24	7.5	7.5	175	7.5	7.5	326	7.498	7.467	477	7.468
25	7.5	7.5	176	7.5	7.5	327	7.498	7.466	478	7.467
26	7.5	7.5	177	7.5	7.5	328	7.498	7.466	479	7.467
27	7.5	7.5	178	7.5	7.5	329	7.498	7.465	480	7.466
28	7.5	7.5	179	7.5	7.5	330	7.498	7.464	481	7.466
29	7.5	7.5	180	7.5	7.5	331	7.498	7.464	482	7.466
30	7.5	7.5	181	7.5	7.5	332	7.498	7.463	483	7.465
31	7.5	7.5	182	7.5	7.5	333	7.498	7.462	484	7.465
32	7.5	7.5	183	7.5	7.5	334	7.498	7.461	485	7.464
33	7.5	7.5	184	7.5	7.5	335	7.498	7.461	486	7.464
34	7.5	7.5	185	7.5	7.5	336	7.498	7.46	487	7.464
35	7.5	7.5	186	7.5	7.5	337	7.498	7.459	488	7.463
36	7.5	7.5	187	7.5	7.5	338	7.498	7.458	489	7.463
37	7.5	7.5	188	7.5	7.5	339	7.498	7.458	490	7.462

38	7.5	7.5	189	7.5	7.5	340	7.497	7.457	491	7.462
39	7.5	7.5	190	7.5	7.5	341	7.497	7.456	492	7.461
40	7.5	7.5	191	7.5	7.5	342	7.497	7.455	493	7.461
41	7.5	7.5	192	7.5	7.5	343	7.497	7.455	494	7.461
42	7.5	7.5	193	7.5	7.5	344	7.497	7.454	495	7.46
43	7.5	7.5	194	7.5	7.5	345	7.497	7.453	496	7.46
44	7.5	7.5	195	7.5	7.5	346	7.497	7.452	497	7.459
45	7.5	7.5	196	7.5	7.5	347	7.497	7.451	498	7.459
46	7.5	7.5	197	7.5	7.5	348	7.497	7.451	499	7.458
47	7.5	7.5	198	7.5	7.5	349	7.497	7.45	500	7.458
48	7.5	7.5	199	7.5	7.5	350	7.497	7.449	501	7.457
49	7.5	7.5	200	7.5	7.5	351	7.497	7.448	502	7.457
50	7.5	7.5	201	7.5	7.5	352	7.496	7.447	503	7.457
51	7.5	7.5	202	7.5	7.5	353	7.496	7.446	504	7.456
52	7.5	7.5	203	7.5	7.5	354	7.496	7.445	505	7.456
53	7.5	7.5	204	7.5	7.5	355	7.496	7.445	506	7.455
54	7.5	7.5	205	7.5	7.5	356	7.496	7.444	507	7.455
55	7.5	7.5	206	7.5	7.5	357	7.496	7.443	508	7.454
56	7.5	7.5	207	7.5	7.5	358	7.496	7.442	509	7.454
57	7.5	7.5	208	7.5	7.499	359	7.496	7.441	510	7.453
58	7.5	7.5	209	7.5	7.499	360	7.496	7.44	511	7.453
59	7.5	7.5	210	7.5	7.499	361	7.496	7.439	512	7.452
60	7.5	7.5	211	7.5	7.499	362	7.495	7.438	513	7.452
61	7.5	7.5	212	7.5	7.499	363	7.495	7.437	514	7.451
62	7.5	7.5	213	7.5	7.499	364	7.495	7.436	515	7.451
63	7.5	7.5	214	7.5	7.499	365	7.495	7.435	516	7.45
64	7.5	7.5	215	7.5	7.499	366	7.495	7.434	517	7.45
65	7.5	7.5	216	7.5	7.499	367	7.495	7.433	518	7.449
66	7.5	7.5	217	7.5	7.499	368	7.495	7.432	519	7.449
67	7.5	7.5	218	7.5	7.499	369	7.495	7.431	520	7.448
68	7.5	7.5	219	7.5	7.499	370	7.495	7.43	521	7.448
69	7.5	7.5	220	7.5	7.499	371	7.494	7.429	522	7.447
70	7.5	7.5	221	7.5	7.499	372	7.494	7.428	523	7.447
71	7.5	7.5	222	7.5	7.499	373	7.494	7.427	524	7.446
72	7.5	7.5	223	7.5	7.499	374	7.494	7.426	525	7.446
73	7.5	7.5	224	7.5	7.499	375	7.494	7.425	526	7.445
74	7.5	7.5	225	7.5	7.499	376	7.494	7.424	527	7.445
75	7.5	7.5	226	7.5	7.499	377	7.494	7.423	528	7.444
76	7.5	7.5	227	7.5	7.499	378	7.493	7.422	529	7.444
77	7.5	7.5	228	7.5	7.498	379	7.493	7.421	530	7.443
78	7.5	7.5	229	7.5	7.498	380	7.493	7.42	531	7.443
79	7.5	7.5	230	7.5	7.498	381	7.493	7.419	532	7.442
80	7.5	7.5	231	7.5	7.498	382	7.493	7.418	533	7.442

81	7.5	7.5	232	7.5	7.498	383	7.493	7.417	534	7.441
82	7.5	7.5	233	7.5	7.498	384	7.493	7.416	535	7.441
83	7.5	7.5	234	7.5	7.498	385	7.492	7.415	536	7.44
84	7.5	7.5	235	7.5	7.498	386	7.492	7.413	537	7.44
85	7.5	7.5	236	7.5	7.498	387	7.492	7.412	538	7.439
86	7.5	7.5	237	7.5	7.498	388	7.492	7.411	539	7.439
87	7.5	7.5	238	7.5	7.498	389	7.492	7.41	540	7.438
88	7.5	7.5	239	7.5	7.497	390	7.492	7.409	541	7.438
89	7.5	7.5	240	7.5	7.497	391	7.491	7.408	542	7.437
90	7.5	7.5	241	7.5	7.497	392	7.491	7.407	543	7.437
91	7.5	7.5	242	7.5	7.497	393	7.491	7.405	544	7.436
92	7.5	7.5	243	7.5	7.497	394	7.491	7.404	545	7.435
93	7.5	7.5	244	7.5	7.497	395	7.491	7.403	546	7.435
94	7.5	7.5	245	7.5	7.497	396	7.491	7.402	547	7.434
95	7.5	7.5	246	7.5	7.497	397	7.49	7.401	548	7.434
96	7.5	7.5	247	7.5	7.496	398	7.49	7.4	549	7.433
97	7.5	7.5	248	7.5	7.496	399	7.49	--	550	7.433
98	7.5	7.5	249	7.5	7.496	400	7.49	--	551	7.432
99	7.5	7.5	250	7.5	7.496	401	7.49	--	552	7.432
100	7.5	7.5	251	7.5	7.496	402	7.489	--	553	7.431
101	7.5	7.5	252	7.5	7.496	403	7.489	--	554	7.43
102	7.5	7.5	253	7.5	7.496	404	7.489	--	555	7.43
103	7.5	7.5	254	7.5	7.495	405	7.489	--	556	7.429
104	7.5	7.5	255	7.5	7.495	406	7.489	--	557	7.429
105	7.5	7.5	256	7.5	7.495	407	7.488	--	558	7.428
106	7.5	7.5	257	7.5	7.495	408	7.488	--	559	7.428
107	7.5	7.5	258	7.5	7.495	409	7.488	--	560	7.427
108	7.5	7.5	259	7.5	7.494	410	7.488	--	561	7.426
109	7.5	7.5	260	7.5	7.494	411	7.488	--	562	7.426
110	7.5	7.5	261	7.5	7.494	412	7.487	--	563	7.425
111	7.5	7.5	262	7.5	7.494	413	7.487	--	564	7.425
112	7.5	7.5	263	7.5	7.494	414	7.487	--	565	7.424
113	7.5	7.5	264	7.5	7.493	415	7.487	--	566	7.423
114	7.5	7.5	265	7.5	7.493	416	7.486	--	567	7.423
115	7.5	7.5	266	7.5	7.493	417	7.486	--	568	7.422
116	7.5	7.5	267	7.5	7.493	418	7.486	--	569	7.422
117	7.5	7.5	268	7.5	7.492	419	7.486	--	570	7.421
118	7.5	7.5	269	7.5	7.492	420	7.486	--	571	7.421
119	7.5	7.5	270	7.5	7.492	421	7.485	--	572	7.42
120	7.5	7.5	271	7.5	7.492	422	7.485	--	573	7.419
121	7.5	7.5	272	7.5	7.491	423	7.485	--	574	7.419
122	7.5	7.5	273	7.5	7.491	424	7.485	--	575	7.418
123	7.5	7.5	274	7.5	7.491	425	7.484	--	576	7.418

124	7.5	7.5	275	7.5	7.491	426	7.484	--	577	7.417
125	7.5	7.5	276	7.5	7.49	427	7.484	--	578	7.416
126	7.5	7.5	277	7.5	7.49	428	7.484	--	579	7.416
127	7.5	7.5	278	7.5	7.49	429	7.483	--	580	7.415
128	7.5	7.5	279	7.5	7.489	430	7.483	--	581	7.415
129	7.5	7.5	280	7.5	7.489	431	7.483	--	582	7.414
130	7.5	7.5	281	7.5	7.489	432	7.482	--	583	7.413
131	7.5	7.5	282	7.5	7.488	433	7.482	--	584	7.413
132	7.5	7.5	283	7.5	7.488	434	7.482	--	585	7.412
133	7.5	7.5	284	7.5	7.488	435	7.482	--	586	7.411
134	7.5	7.5	285	7.5	7.487	436	7.481	--	587	7.411
135	7.5	7.5	286	7.5	7.487	437	7.481	--	588	7.41
136	7.5	7.5	287	7.5	7.487	438	7.481	--	589	7.41
137	7.5	7.5	288	7.5	7.486	439	7.48	--	590	7.409
138	7.5	7.5	289	7.5	7.486	440	7.48	--	591	7.408
139	7.5	7.5	290	7.5	7.486	441	7.48	--	592	7.408
140	7.5	7.5	291	7.5	7.485	442	7.48	--	593	7.407
141	7.5	7.5	292	7.5	7.485	443	7.479	--	594	7.406
142	7.5	7.5	293	7.499	7.484	444	7.479	--	595	7.406
143	7.5	7.5	294	7.499	7.484	445	7.479	--	596	7.405
144	7.5	7.5	295	7.499	7.484	446	7.478	--	597	7.405
145	7.5	7.5	296	7.499	7.483	447	7.478	--	598	7.404
146	7.5	7.5	297	7.499	7.483	448	7.478	--	599	7.403
147	7.5	7.5	298	7.499	7.482	449	7.477	--	600	7.403
148	7.5	7.5	299	7.499	7.482	450	7.477	--	601	7.402
149	7.5	7.5	300	7.499	7.481	451	7.477	--	602	7.401
150	7.5	7.5	301	7.499	7.481	452	7.476	--	603	7.401
151	7.5	7.5	302	7.499	7.48	453	7.476	--	604	7.4

Temperature changing progress at abstraction level
(Contrary flow, intermittent operation)

Day 1

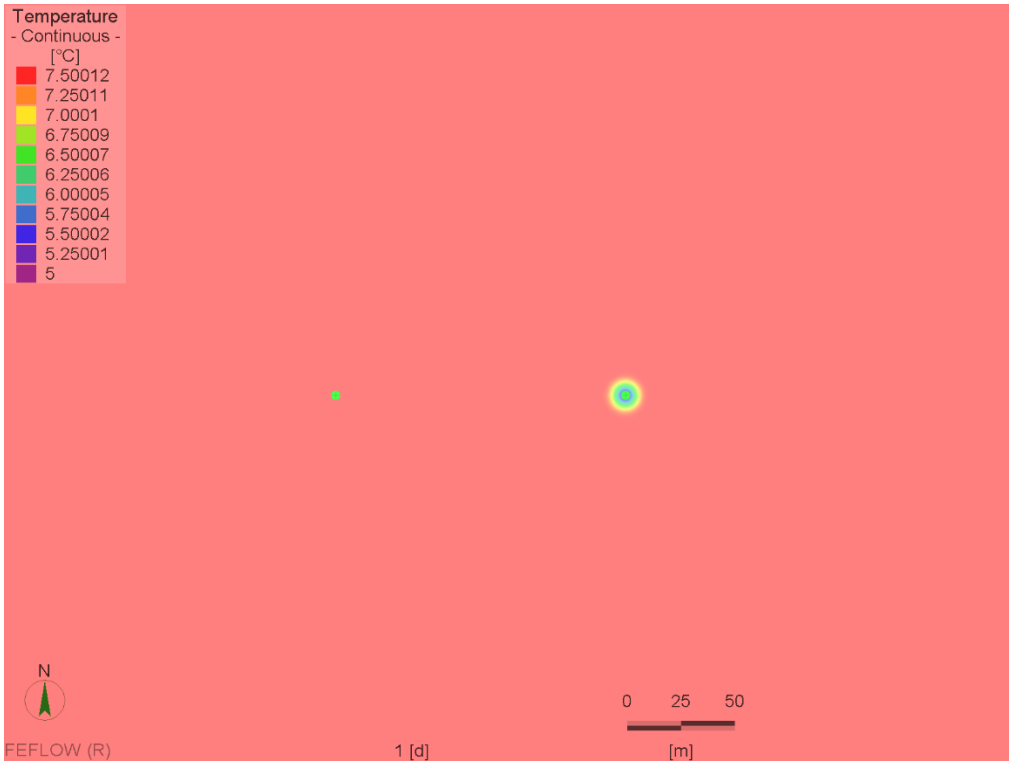

Day 10

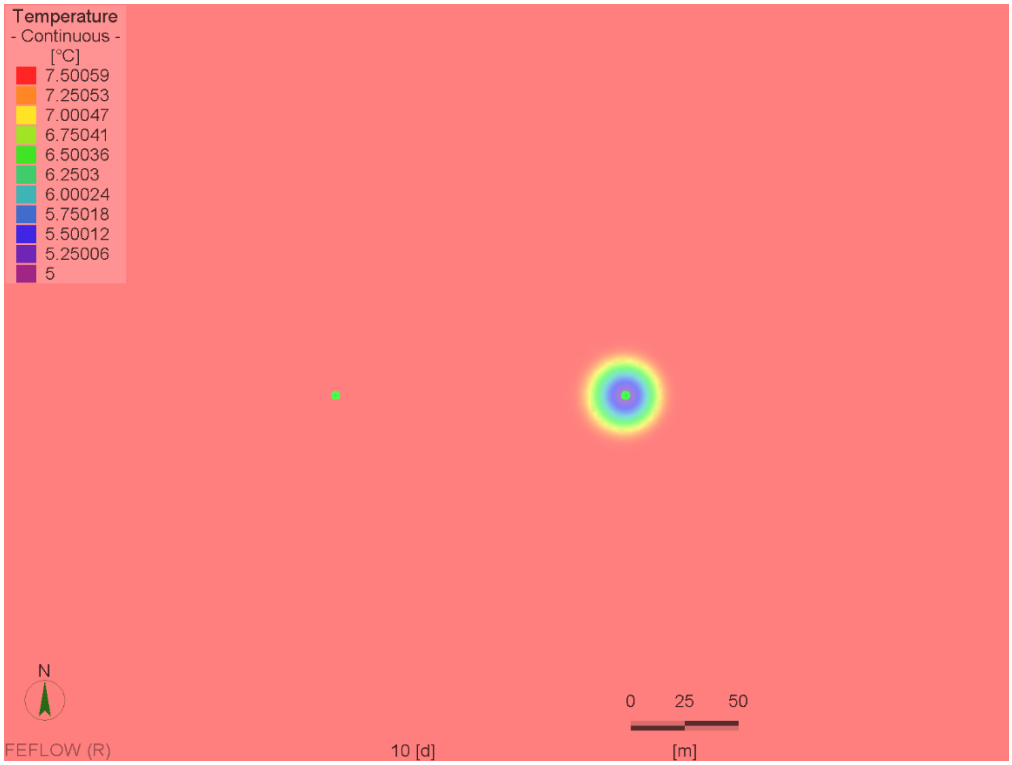

Day 100

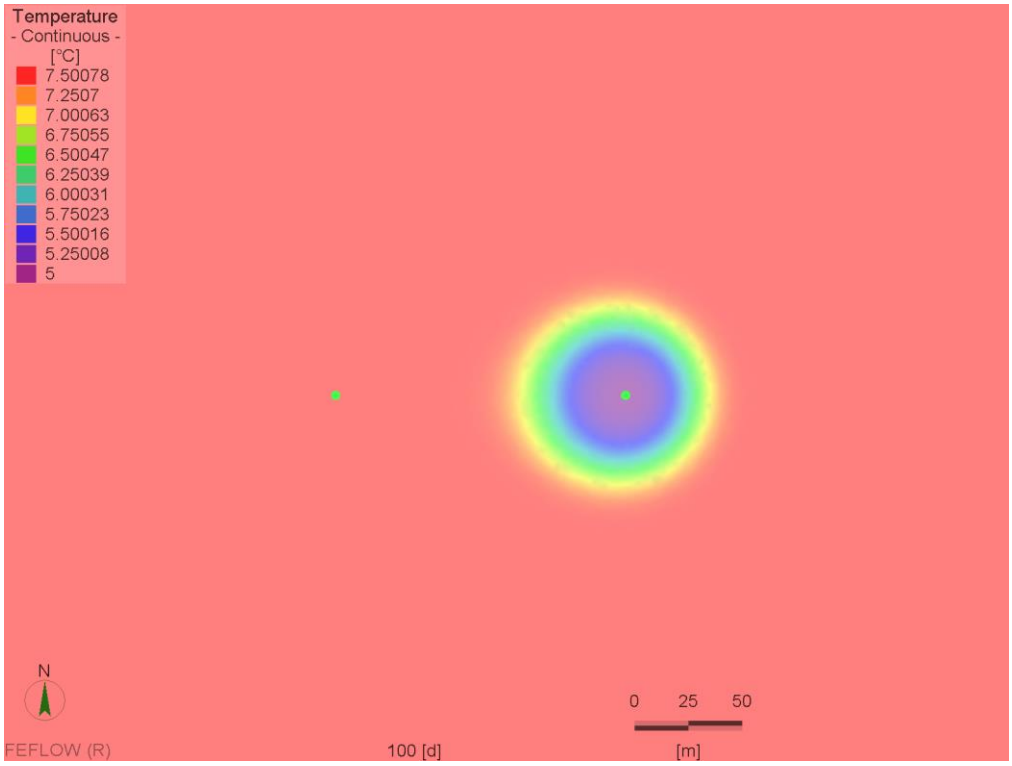

Day 240 （The last day of operation in year 1, the system is going to be put into a halt for the coming 125 days）

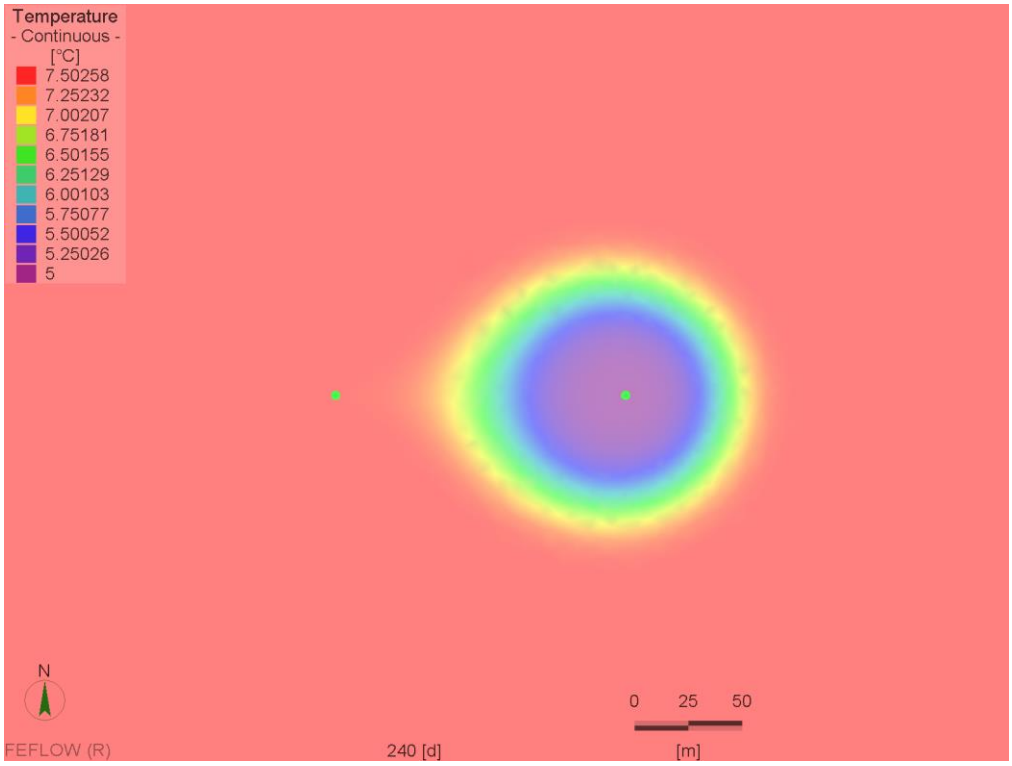

Day 365 (The last of year 1, the GWHP system is going to be put into operation again)

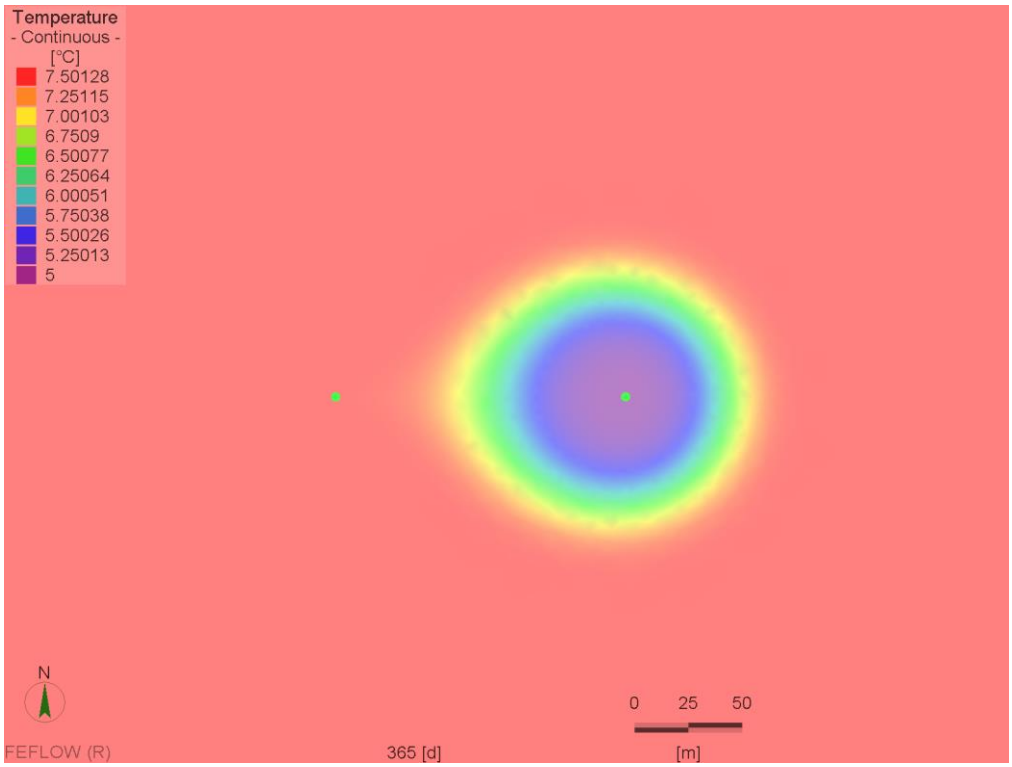

Day 365 (Thermal breakthrough day)

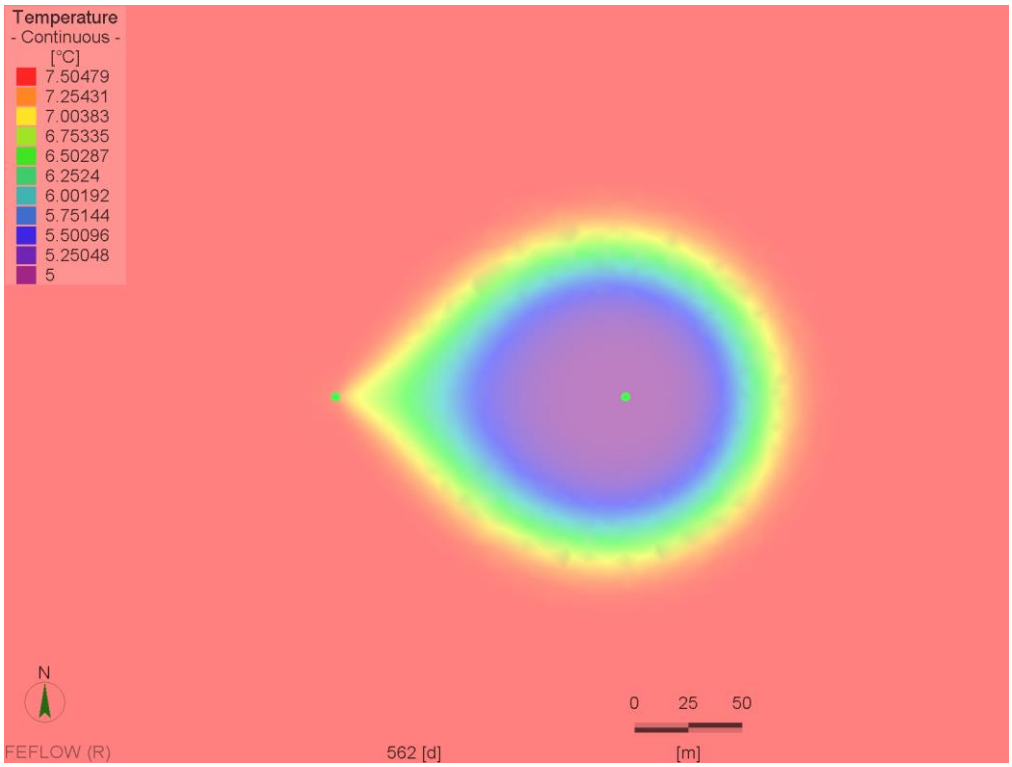

Day 3650 (Final day of simulation)

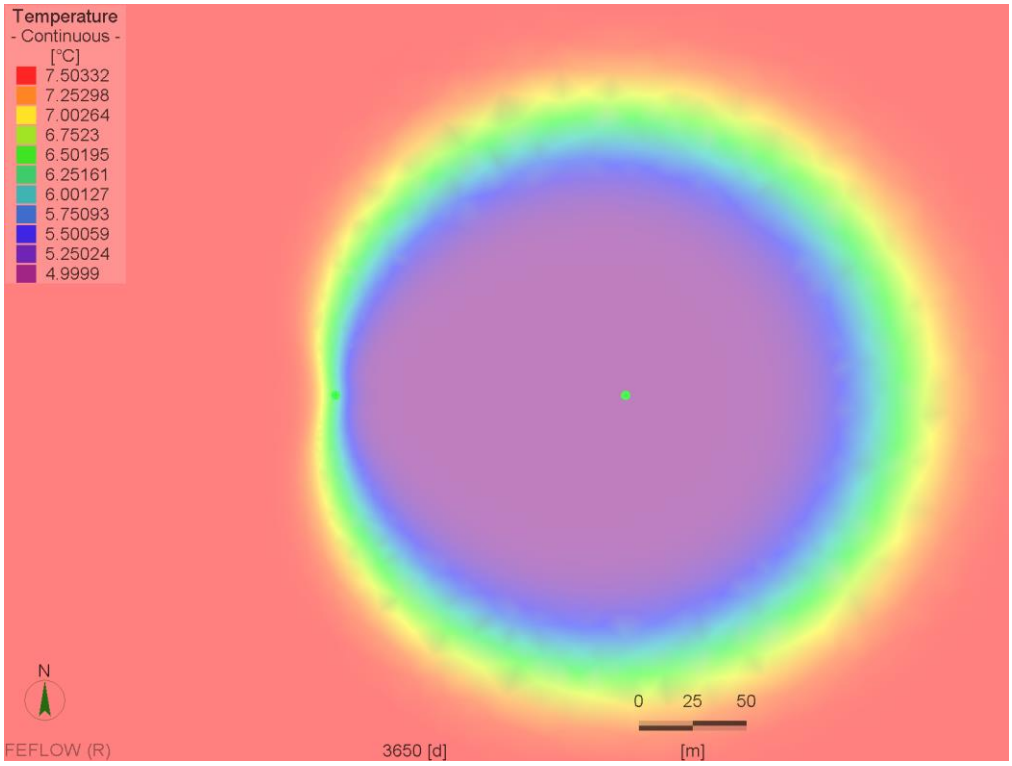
Temperature
- Continuous -
[°C]
7.50332
7.25298
7.00264
6.7523
6.50195
6.25161
6.00127
5.75093
5.50059
5.25024
4.9999
N
0
25
50
FEFLOW (R)
3650 [d]
[m]